AD-A041 179 NAVAL POSTGRADUATE SCHOOL MONTEREY CALIF F/G 20/4
FORCES ON ROUGHENED CYLINDERS IN HARMONIC FLOW AT HIGH REYNOLDS--ETC(U)
SEP 76 S R EVANS

UNCLASSIFIED NL

1 OF 1
AD A041179

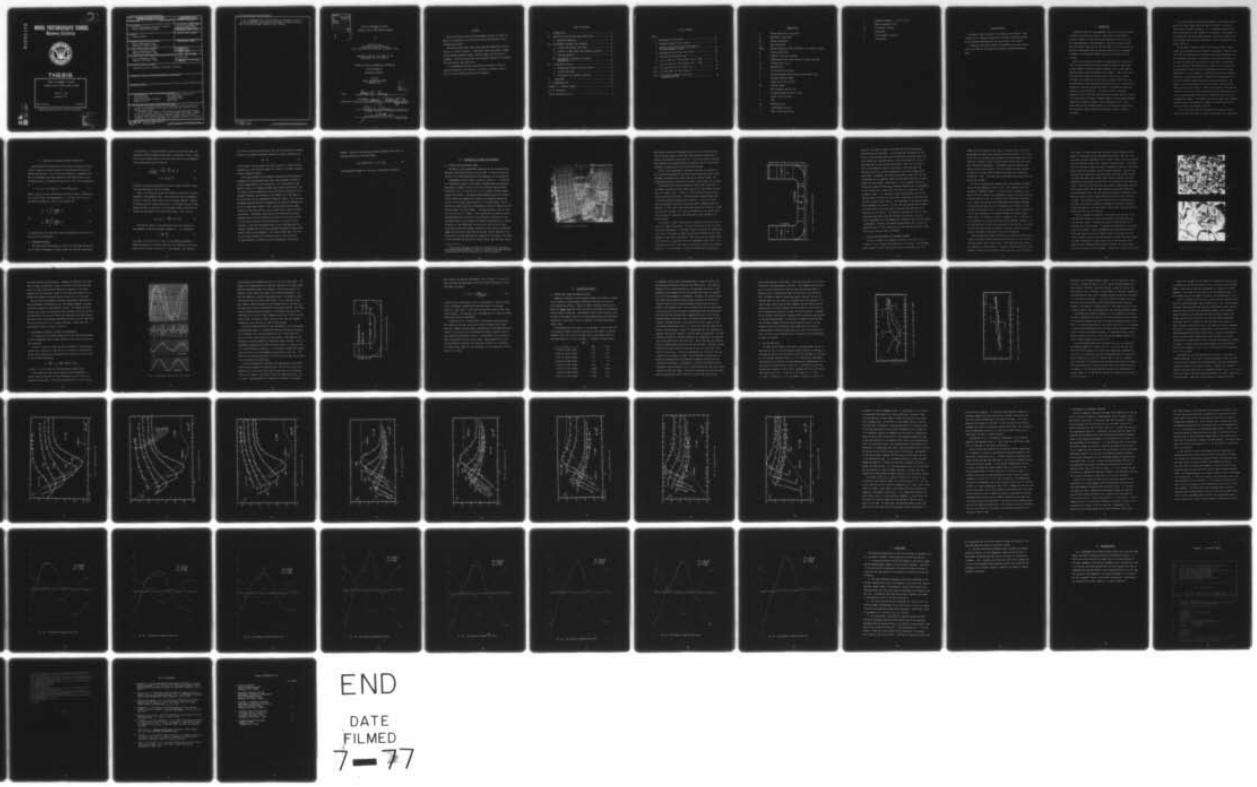

END

DATE FILMED
7-77

NAVAL POSTGRADUATE SCHOOL
Monterey, California

THESIS

FORCES ON ROUGHENED CYLINDERS
IN
HARMONIC FLOW AT HIGH REYNOLDS NUMBERS

by

Steven R. Evans

September 1976

Thesis Advisor: T. Sarpkaya

Approved for public release; distribution unlimited.

SECURITY CLASSIFICATION OF THIS PAGE (When Data Entered)

REPORT DOCUMENTATION PAGE		READ INSTRUCTIONS BEFORE COMPLETING FORM
1. REPORT NUMBER	2. GOVT ACCESSION NO.	3. RECIPIENT'S CATALOG NUMBER
4. TITLE (and Subtitle) Forces on Roughened Cylinders in Harmonic Flow at High Reynolds Numbers		5. TYPE OF REPORT & PERIOD COVERED Engineer's and Master's Thesis; September 1976
		6. PERFORMING ORG. REPORT NUMBER
7. AUTHOR(s) Steven R. Evans		8. CONTRACT OR GRANT NUMBER(s)
9. PERFORMING ORGANIZATION NAME AND ADDRESS Naval Postgraduate School Monterey, California 93940		10. PROGRAM ELEMENT, PROJECT, TASK AREA & WORK UNIT NUMBERS
11. CONTROLLING OFFICE NAME AND ADDRESS Naval Postgraduate School Monterey, California 93940		12. REPORT DATE September 1976
		13. NUMBER OF PAGES 72
14. MONITORING AGENCY NAME & ADDRESS(if different from Controlling Office) Naval Postgraduate School Monterey, California 93940		15. SECURITY CLASS. (of this report) Unclassified
		15a. DECLASSIFICATION/DOWNGRADING SCHEDULE

16. DISTRIBUTION STATEMENT (of this Report)

Approved for public release; distribution unlimited.

17. DISTRIBUTION STATEMENT (of the abstract entered in Block 20, if different from Report)

18. SUPPLEMENTARY NOTES

19. KEY WORDS (Continue on reverse side if necessary and identify by block number)

In-line Forces
Oscillatory Flow
Harmonic Flow about Cylinders
Rough Cylinders
Drag and Inertia Coefficients
Lift Coefficient
Alternating Force
Wave Forces

20. ABSTRACT (Continue on reverse side if necessary and identify by block number)

The in-line forces acting on sand-roughened circular cylinders immersed in an harmonically oscillating flow have been measured using a U-shaped water tunnel.

The drag and the inertia coefficients have been determined through the use of a Fourier analysis. These coefficients were found to depend on the Keulegan-Carpenter number, Reynolds number, and the relative roughness. The results have shown that roughness dramatically increases the transcritical drag coefficient.

DD FORM 1 JAN 73 1473 (Page 1) EDITION OF 1 NOV 65 IS OBSOLETE S/N 0102-014-6601

SECURITY CLASSIFICATION OF THIS PAGE (When Data Entered)

It is recommended that the experiments be extended to the self-excited hydroelastic oscillations of cylinders in harmonic flows as well as to the problems related to wave slamming.

Forces on Roughened Cylinders in Harmonic Flow at High Reynolds Numbers

by

Steven R. Evans
Lieutenant, United States Navy
B.S., University of Mississippi, University, 1969

Submitted in partial fulfillment of the
requirements for the degree of

MASTER OF SCIENCE IN MECHANICAL ENGINEERING

and the degree of

MECHANICAL ENGINEER

from the

NAVAL POSTGRADUATE SCHOOL
September 1976

Author Steven R. Evans

Approved by: Thesis Advisor

Chairman, Department of Mechanical Engineering

Academic Dean

ABSTRACT

The in-line forces acting on sand-roughened circular cylinders immersed in an harmonically oscillating flow have been measured using a U-shaped water tunnel.

The drag and the inertia coefficients have been determined through the use of a Fourier analysis. These coefficients were found to depend on the Keulegan-Carpenter number, Reynolds number, and the relative roughness. The results have shown that roughness dramatically increases the transcritical drag coefficient.

It is recommended that the experiments be extended to the self-excited hydroelastic oscillations of cylinders in harmonic flows as well as to the problems related to wave slamming.

TABLE OF CONTENTS

LIST OF FIGURES

NOMENCLATURE

A	Virtual amplitude of the motion
A_1	Amplitude of the motion
a_m	Maximum acceleration
C_d	Drag coefficient
CLMAX	Maximum transverse force coefficient, also used as C_L (max)
C_m	Inertia coefficient
D	Diameter of the test cylinder
F	Instantaneous total force acting on the test cylinder
f_r	Frequency ratio $f_v/1/T$
F_m	Measured force
g	Gravitational acceleration
H	Distance between pressure taps and mean water level
K	Keulegan-Carpenter number
L	Length of the test cylinder
Re	Reynolds number
k	Sand roughness particle size
s	Distance between the pressure taps
T	Period of oscillations
t	Time
U_m	Maximum velocity
u	Instantaneous velocity
w	Width of the test section

β	Frequency parameter, $\beta = D^2/\nu T = Re/K$.
γ	Specific weight of fluid
Δp	Differential pressure
θ	Phase angle
ν	Fluid kinematic viscosity
ρ	Fluid density

ACKNOWLEDGEMENT

The author wishes to extend a warm thank-you to Professor Turgut Sarpkaya for his thorough guidance and invaluable assistance throughout the detailed experimentation and the editing of this thesis.

In addition, the author wishes to acknowledge the careful efforts of Mr. Jack McKay of the Mechanical Engineering Department Machine Shop.

I. INTRODUCTION

Information about the time-dependent forces acting on bluff bodies in general and circular cylinders in particular has considerable practical interest in ocean and wind engineering, as well as in the basic understanding of fluid mechanics. Extensive discussion about the flow-induced forces and oscillations exists in the literature, but the basic hydrodynamic data are lacking, particularly for roughened cylinders at high Reynolds numbers which are of current practical interest.

Much of the present knowledge on the hydrodynamics of the oscillatory flow about cylinders has been obtained by means of model tests in wave channels at Reynolds numbers generally two to three orders of magnitude smaller than prototype Reynolds numbers. These model tests, which have been primarily concerned with in-line forces on smooth cylinders, have disclosed that the drag and inertia coefficients may be correlated with the amplitude of motion relative to a characteristic dimension of the body and that the effect of the Reynolds number was obscured by that correlation. The results recently reported by Sarpkaya [1] and Collins [2] have shown that the drag, inertia, and the lift coefficients for smooth cylinders depend on the Keulegan-Carpenter number and the Reynolds number. These investigators have clearly established the relationship between the force-transfer coefficients, the Keulegan-Carpenter number and the Reynolds number for smooth cylinders.

It is a well known fact that the structures in the ocean environment do not remain smooth and that they are covered in time with rigid as well as soft excrescences. It is therefore important that not only the effect of the increase in the diameter of the members of a structure but also the roughness effect of the marine growth on the force-transfer coefficients be determined in order to establish safe design criteria.

Of the scores of papers written on the drag and inertia coefficients, none have dealt with the effect of roughness. Ordinarily one would like to investigate this problem in the ocean environment or in the laboratory with waves. Experiments in the ocean environment are not easy to conduct and are subject to a great deal of uncertainty not only because of the random nature of waves, but also because of the presence of currents and the three-dimensional nature of waves. Experiments in a wave channel in a laboratory are not very meaningful because it is almost impossible to generate high enough waves which will yield Reynolds numbers approaching those encountered in the oceans. It is partly because of the difficulties cited above and partly because of the desire to control the parameters affecting the variation of the force coefficients that the experiments were carried out in a two-dimensional flow situation through the use of a large U-shaped water tunnel. Furthermore, the test cylinders were roughened with sand of uniform diameter in a manner to be described later in order to control the roughness condition.

It is a well known fact that roughness brings about an earlier drag crisis and gives rise to a higher transcritical drag coefficient

for rough cylinders in steady uniform flow. Experiments of Fage and Warsap [3] and Achenbach [4] have shown that roughness retards the boundary layer and the separation point because of higher skin friction thereby increasing the size of the wake and the drag coefficient. They have also shown that roughness, because of the disturbances generated, causes an earlier transition in the shear layers and precipitates the occurrence of the drag crisis. The combination of these phenomena, namely the retardation of the separation points and the earlier occurrence of the drag crisis, yields a minimum drag coefficient which is higher than that for a smooth cylinder. In fact, the larger the roughness, the larger the minimum drag coefficient and the smaller the Reynolds number at which that minimum occurs. It is on the basis of these measurements that one would anticipate a similar behavior in harmonic flows as far as the effect of roughness is concerned. In fact, for a long time it has been assumed in the offshore industry that the effect of roughness in wavy flows will be identical to that observed in steady flows. Such a practice assumes that the transcritical drag coefficient depends only on the relative roughness and the representative Reynolds number and is independent of the character of the ambient flow. Both in wavy flows and in two-dimensional harmonic flows, the wake of the cylinder changes its position with time, and the flow pattern about the cylinder is considerably more complex than that in steady flow. Furthermore, in the absence of any reliable data, there is no reason to assume that the effect of roughness in harmonic flow will be identical to that in steady flow.

It is for the reasons cited above that an extensive investigation of the effect of roughness on the force-transfer coefficients for circular cylinders immersed in harmonic flow has been undertaken. The drag and inertia coefficients have been determined for a wide range of Keulegan-Carpenter numbers, Reynolds numbers, and relative sand roughnesses.

II. ANALYSIS OF THE DATA AND FORCE COEFFICIENTS

Data reduction for the forces in-line with the direction of oscillation is based on a Fourier analysis of the measured force and the Morison equation [5]. The in-line force exerted on a submerged cylinder in an unsteady flow, which consists of the inertia force F_i and the drag force F_d, is assumed by Morison, et al. [5], to be expressible by

$$F = F_d + F_i = 0.5\, C_d LD\rho U|U| + 0.25\, \pi\rho LD^2 C_m\, dU/dt \qquad (1)$$

where C_d and C_m are the coefficients of drag and inertia, respectively. For an oscillating flow represented by $U = -U_m \cos\theta$, with $\theta = 2\pi t/T$, the Fourier averages of C_d and C_m are given by [6].

$$C_d = -\frac{3}{4} \int_0^{2\pi} \frac{F \cos\theta}{\rho U_m^2 LD}\, d\theta \qquad (2)$$

and

$$C_m = \frac{2U_m T}{\pi^3 D} \int_0^{2\pi} \frac{F \cos\theta}{\rho U_m^2 LD}\, d\theta \qquad (3)$$

All quantities on the right-hand side of the equations (2) and (3) are known or are to be measured.

A. GOVERNING PARAMETERS

The coefficients cited above will have to be correlated through the use of suitable parameters in order to show that they have some degree

of universality. A simple dimensional analysis of the flow under consideration (uniform harmonic motion about a roughened circular cylinder with its axis placed normal to the flow) shows that the time-dependent force coefficients may be written as:

$$\frac{F}{0.5\rho DLU_m^2} = f\left(\frac{U_m T}{D}, \frac{U_m D}{\nu}, \frac{k}{D}, \frac{t}{T}\right) \tag{4}$$

$$= f\left(K, Re, \frac{k}{D}, \frac{t}{T}\right) \tag{5}$$

Evidently, $U_m T/D$ may be replaced by $2\pi A/D$ or simply A/D where A represents the amplitude of the oscillations.

There is no simple way to deal with equation (5) even for the most manageable time-dependent flows. The evaluation of the instantaneous values of the force coefficients is not at present feasible. Another and perhaps the only other alternative is to eliminate time as an independent variable in equation (5) and consider suitable time-invariant averages or amplitudes of the force coefficients. Thus, one has

$$[C_d, C_m] = f_i\left(\frac{U_m T}{D}, Re, k/D\right) \tag{6}$$

The Reynolds number in the above equation may be replaced by a new parameter called the frequency parameter, β. It is defined as

$$\beta = \frac{Re}{K} = \frac{D^2}{\nu T} \tag{7}$$

The reason for the use of β is that, in the present experiments, it remains constant for a given cylinder and fluid temperature since the period of oscillation is fixed at T = 5.507 seconds. The variation

of any one of the force coefficients with K may be plotted for constant values of β and then the Reynolds number may be easily recovered from

$$Re = \beta K \tag{8}$$

In this manner, one can connect the points on each β = *constant curve*, representing a given Reynolds number for a family of suitably selected values of Reynolds numbers.

It has been assumed in the foregoing discussion that the effect of roughness could be characterized by the single parameter k/D where k is the average height of the sand grains. It is known that [7] the physical height of a roughness element could differ significantly from its effective height depending on the distribution and packing of the roughness elements, the character of the ambient flow, the shape of the bluff body, and the representative Reynolds number. Thus, the one-parameter characterization of roughness must be done with extreme care. As will be described in detail later, the sand particles have been carefully sieved and applied to the cylinders with as much uniformity as possible. Furthermore, the packing of the sand grains has been examined under a scanning electron microscope so as to insure uniformity and quality control of the distribution of the grains on the cylinders. With such precautions taken, it was considered that the relative roughness will be the most important parameter reflecting the overall effect of the roughness. This view has been amply justified by the results obtained with different sizes of sand grains and cylinder diameters at identical relative roughnesses and Reynolds

numbers. Suffice it to note that the data reported herein shall be analyzed according to the relationship

$$C_i[\text{a coefficient}] = f_i(K, \beta, \frac{k}{D}) \tag{9}$$

and the Reynolds number will be used in the manner cited above.

III. EXPERIMENTAL EQUIPMENT AND PROCEDURES

A. U-SHAPED OSCILLATING-FLOW TUNNEL

The details of the experimental apparatus and the procedures were previously described in detail in [1] and [8]. In the following discussion, only a brief description of the apparatus will be presented.

A photograph of the U-tunnel is shown in figure (1). It consists of 11 modules for ease of construction, transportation, and mounting. Each module is made of 0.05 cm (3/8 inch) aluminum plates and reinforced with 1.27 x 10 x 46 cm (1/2 x 4 x 18 inches) aluminum flanges welded to the plates. The modules were assembled using an air drying silicon rubber seal between the flanges of two adjacent modules and 2.54 cm (1 inch) steel bolts placed 15 cm (6 inches) apart. The inside of each module was precision machined so that the largest misalignment was about 1 mm (0.04 inches). The cross-section of the two legs is 183 x 91.5 cm (6 x 3 feet). This selection was dictated by several considerations such as available ceiling height, pressures to be encountered (hence, the structural and economic considerations), a desire to obtain a virtual amplitude* or velocity of oscillation at least twice that of the free surface, the period of oscillation, the Reynolds number and the relative amplitude A/D desired, natural damping of the oscillations, and the magnitude and frequency of the forces. The length of the horizontal test section was chosen larger than twice the virtual

---

*The virtual amplitude is defined as the amplitude of oscillation which the cylinder experiences. Here it is exactly twice the amplitude of oscillation of the free surface in one leg of the tunnel.

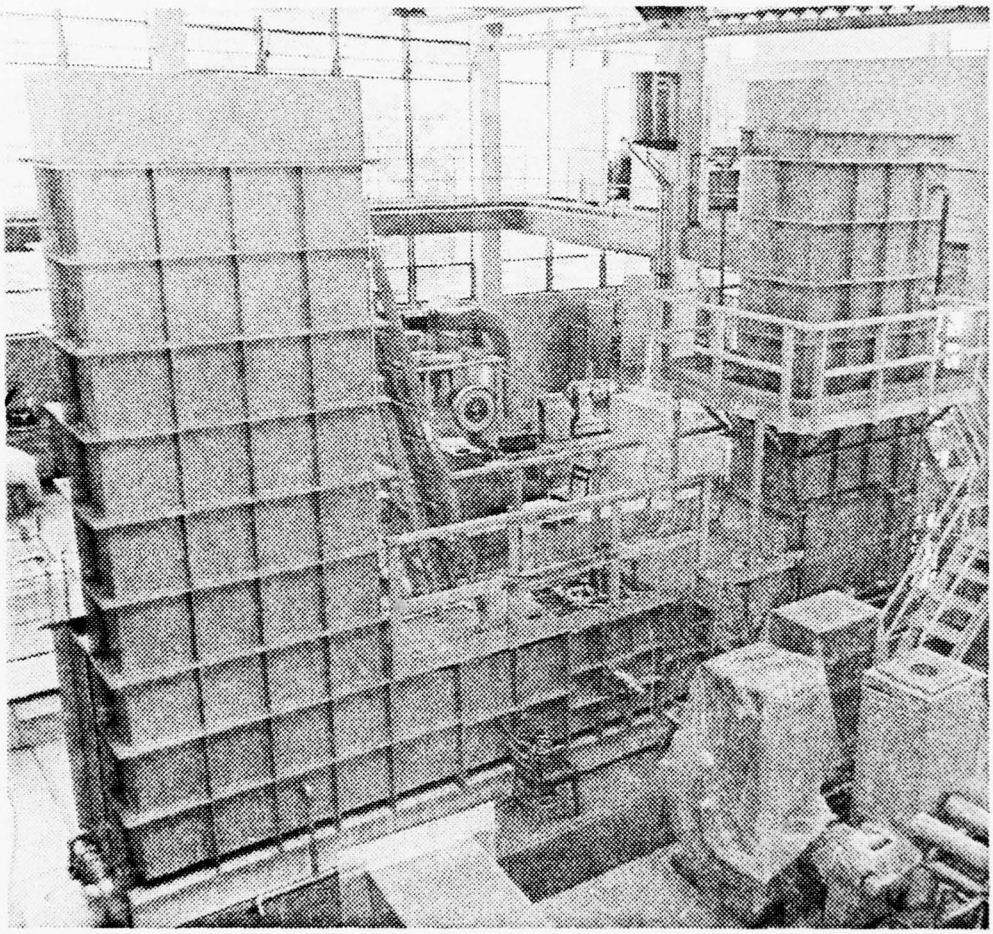

Fig. 1 Photograph of the U-tunnel

amplitude to insure fully developed uniform flow at the test section. Finally the two corners of the tunnel were carefully streamlined to prevent flow separation (see figure 2). This design proved to be more than adequate for no separation was encountered, and also the desired frequency and amplitude of oscillation were achieved.

The auxiliary components of the tunnel consisted of plumbing for the filling and emptying of the tunnel with hot and cold water, a heat exchanger, butterfly-valve system, and the air supply system. The plumbing consisted of simple piping, valves, a small pump, and a filter.

The butterfly-valve system (mounted on top of one of the legs of the tunnel) consisted of four plates, each 4.6 cm (18 inches) wide and 92 cm (36 inches) long. A 2.54 cm (1 inch) steel shaft was placed at the axis of each valve plate. Aluminum housings supported both ends of the shaft with self-aligning ball bearings. A 15 cm (6 inches) gear was attached to one end of each shaft which extended beyond the bearing. All four valve plates were then aligned and driven by a simple rack and pinion system. The rack was actuated by an air-driven piston with the help of a three-way valve connected to the laboratory air supply system.

The valves, in their closed position, completely sealed the top of one of the legs of the tunnel. The top of the other leg was left open. Initially, the butterfly valves were closed, and the air was admitted to that side of the tunnel to create the desired differential water level between the two legs of the tunnel. Then the valves were opened quickly with the help of a pneumatically-driven three-way control valve. This action set the fluid in the tunnel in oscillatory motion with a natural period of $T = 5.507$ seconds. A series of experiments was conducted

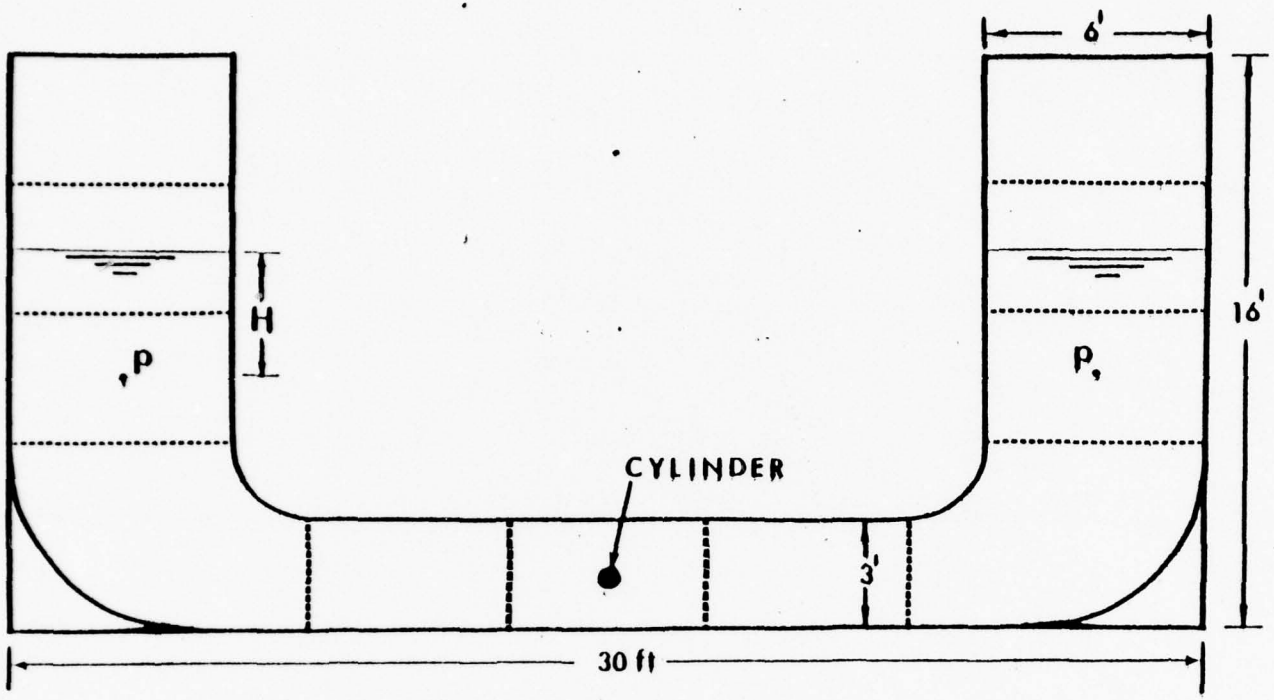

Fig. 2 Schematic Drawing of the U-tunnel.

with one of the test cylinders to evaluate some of the experimental characteristics of the tunnel. It was found that the damping of the motion is such that the amplitude of oscillations decreases about 3 mm (0.12 inches) per cycle and about 0.15 mm (0.06 inches) per cycle for amplitudes half or less than of the maximum. Thus, over a period of four or five complete cycles of oscillation at any amplitude, the amplitude, velocity, and the acceleration of the fluid changed about one percent. Evidently, the forced oscillations of the fluid, if such a method were to be employed, cannot yield the amplitude to an accuracy better than one percent. Additionally, in such a method, one has to contend with some high frequency vibrations, however small, superimposed on the acceleration. These result from the cyclic operation of the butterfly valves. It is because of these considerations that the experiments were carried out by letting the system damp out the amplitude over many cycles of oscillations. The advantages of the method adopted become apparent very quickly. Firstly, the oscillations were so smooth and quiet that one could not know or even hear that 5000 gallons of water were in oscillation. The elevation, acceleration, and all force traces were absolutely free from secondary oscillations so that no filters whatsoever were used between the transducer output and the recording equipment. Secondly, the method adopted enables one to cover all possible values of K for a given β and k/D and see the evolution of the forces over a period of about 30 minutes.

B. CIRCULAR CYLINDER MODELS AND ROUGHNESS ELEMENTS

Circular cylinders with diameters ranging in size from 17.5 cm (7 inches) to 5 cm (2 inches) have been used in this study. The cylinders were turned on a lathe from aluminum pipes or plexiglass rods. The

length of each cylinder was such that it allowed 0.08 cm (1/32 inch) gap between the tunnel wall and each end of the cylinder. As will be noted later, the cylinder was prevented from moving towards one or the other wall by means of small O-rings attached to the round cantilever end of the force transducers. A doubleball precision bearing (SKF-2303-J) with an approximatley 1.5 cm (0.6 inches) bore was inserted at each end of the cylinder in aluminum housings which sealed the cylinder air tight. The other face of each bearing was flush with the end of the cylinder.

In view of the discussion concerning the one-parameter characterization of the roughness in terms of k/D, it was decided to use only one type of roughness element. The possible use of sandpaper, glass beads, and wire screens was disregarded for they would have exhibited different packing as well as different size distribution characteristics. Clean sand obtained from the Monterey Sand Company, Monterey, CA, was sieved through the use of standard A.S.T.M. sieves in order to obtain a given grain size. It must be emphasized that a particular size of sand represents a distribution between two closely spaced sieve sizes. For example, a relative roughness of k/D = 1/400 may in fact represent for a given cylinder an average between 1/380 and 1/410. Considering the fact that the distribution of the sand over a cylinder may vary from one cylinder to another, the range of the size distribution cited above is considered to be quite acceptable.

Each cylinder was mounted horizontally on a specially constructed, manually operated, rotating apparatus and covered with a thin layer of air-drying epoxy resin using a brush. Even though the description of the technique is rather simple, it required a certain amount of craftsmanship to obtain a uniform coat of epoxy resin which did not contain

thick spots or surface waves. When the epoxy coating reached a certain degree of consistency and was considered satisfactory, then the finely pre-sieved sand was transferred into a slightly larger sieve and sprinkled over the rotating cylinder from a height of about 6 inches. In the meantime, the cylinder surface was visually inspected to make sure that there were no open spots anywhere, nor any foreign substances. Upon the completion of the sprinkling of the sand, the cylinder was slowly rotated to prevent the epoxy from flowing. Within about 10 minutes, the epoxy hardened and the cylinder was left alone for the epoxy to cure (about 24 hours). Then the cylinder surface was cleaned to remove excess sand and extra sand particles that at times attached to each other forming an easily breakable spike. This was done not by hand but rather by firmly holding a piece of plastic paper against the surface of the rotating cylinder. This procedure has been followed for all cylinders and has invariably resulted in cylinders of roughness with perfect uniformity. Sample photographs of the rough surface, taken with a scanning electron microscope, are shown in figure (3).

Prior to mounting the cylinder in the tunnel, the two ends of the cylinder were cleaned to remove excess patches of any epoxy that may have been left there. The bearings previously described were then inserted into their housings. To complete the description of the mounting of the cylinder, it must be emphasized that extraordinary precautions were taken so as not to damage any part of the rough surface. For this purpose, the cylinder was completely wrapped with plastic paper and then transported to a wide canvas sling inside the test section. Then the force transducers were properly inserted, the sling removed, and all the mounting bolts tightened. Finally, the cylinder was slightly

k = 0.018"
20-X

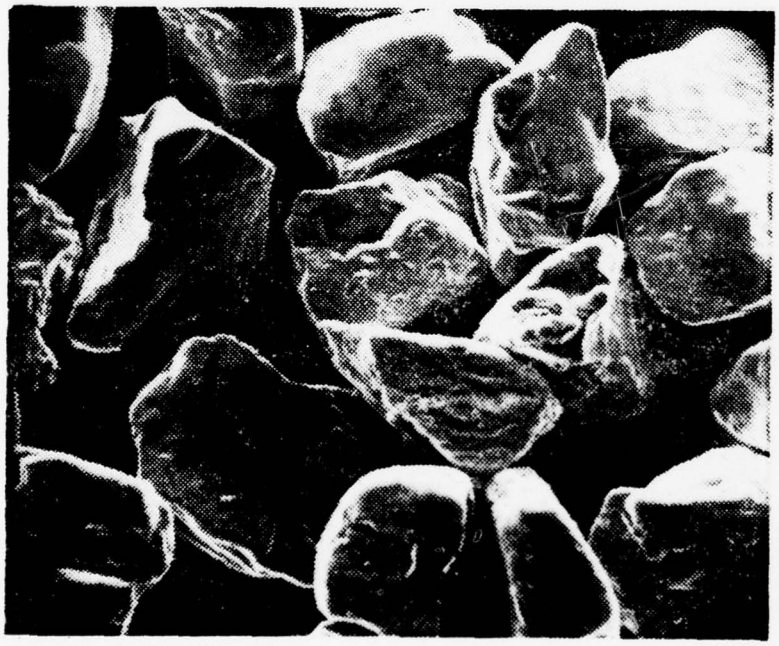

k = 0.018"
50-X

Fig. 3 Scanning Electron Microscope Photographs of sand-roughened surface

moved by hand to insure that it was freely and properly mounted onto the force transducers.

In order to determine the variation of the force coefficients with Reynolds number for a given Keulegan-Carpenter number and relative roughness, all cylinders were tested at the same relative roughnesses (k/D = 1/800, 1/400, 1/200, 1/100, and 1/50), and the experiments were carried out at three water temperatures (at about 55°, 95°, 120°). The enormous heat capacity of the tunnel and the fluid helped to maintain a constant, uniform temperature. The expansion of the test cylinders was less than 1/32 inches (0.8 mm) at the highest temperature tested.

C. FORCE MEASUREMENTS

Two identical force transducers, one at each end of the cylinder, were used to measure the instantaneous in-line and transverse forces. The basic transducer was manufactured by B.L.H. Electronics, Inc., under the trade name LBP-1 and catalogue no. 420271. The gage has a capacity of 224 N (500 Lbf) with an overload capacity of 200 percent. The deflection of the gage under 500 Lbf load was 0.25 mm (0.01 inch). For the largest cylinder and amplitude encountered in the experiments, the maximum load was less than 200 Lbf, and the deflection of the beam was less than 0.2 mm (0.008 inches).

A special housing was built for each gage so that it could be mounted on the tunnel window and rotated to measure either the in-line or the transverse force alone. The bellows which protected the strain gages had to be waterproofed in such a manner that they would not adversely affect the operation of the gages when subjected to about 6 m (20 feet) water pressure at temperatures 18 C (64 F) to 74 C (165 F). For this purpose the bellows were completely filled with Dow Corning

3140 - RTV coating without bringing the rubber into contact with air during the filling operation. After filling, the ends of the bellows were sealed air tight with special clamps. The silicon rubber remained in its original liquid form throughout the operation of the gages.

After the mounting of the first cylinder, the exact angular position of the gages within their housing had to be determined and set with a pin so that the gages measure either only the in-line or the transverse force. For this purpose, an approximatley 400 N load was hung on the cylinder with a lubricated nylon rope. The in-line force (acting in the horizontal direction) was observed on the amplifier recorder system. Then the gage was rotated in small increments until the in-line force was exactly zero. A final check was made by measuring the outputs of the gages with a precision voltmeter. The position of each gage was marked and set with a pin. Finally, four bolts were placed on the gage housing to hold the gages rigidly in position. Removal of these bolts and the pin allowed the rotation of the gages exactly 90 degrees, after which the bolts and pin were placed in position. In this manner the gages were capable of measuring either the in-line or the transverse force without any "cross talk" between the in-line and transverse forces. Ordinarily, one gage was set to measure in-line force and the other gage, the transverse force. At times both gages were used to measure only the in-line or the transverse force.

The calibration of each gage was accomplished by hanging loads in the middle of the cylinder after setting both gages to sense only the transverse (here vertical) force. The directional sensitivity of the gages was also checked by applying identical loads upwards on the test cylinders with the help of a hook-cantilever arm attached to the top of

the tunnel outside the test section. Repeated calibrations have shown that the gages are perfectly linear up to 2000 N; they yield the same signal for loads applied either downward or upwards; and the gages, together with the electronic system to which they were eventually connected, were capable of sensing forces as small as 0.1 N (0.02 Lbf).

The in-line and transverse force were simultaneously recorded with the instantaneous acceleration on two two-channel Honeywell recorders running at a speed of 10 divisions per second. This speed gave 55.07 divisions per cycle. The amplitude of the transverse force and the flow characteristics such as $U_m T/D$ and Re were determined from these traces. RMS value of the lift force was determined for each cycle by reading the force at every division or 0.1 second intervals. Sample force and acceleration traces are shown in figure 4.

D. ACCELERATION, ELEVATION, OR VELOCITY MEASUREMENTS

It is because of the extreme importance of the accurate measurement of the instantaneous value of these quantities that they are discussed here separately.

Firstly, it should be noted that the measurement of the amplitude, acceleration, elevation, or the velocity is a matter of interpretation of the signal received from the appropriate transducer in light of one of the following expressions

$$U_m = \frac{2\pi A}{T}, \quad a_m = \frac{dU}{dt} = \left(\frac{2\pi}{T}\right)^2 A = \frac{2\pi}{T} U_m$$

in which T = 5.507 seconds for the experiments reported here.

Three transducers were used to generate three independent d.c. signals, each proportional to the instantaneous value of one of the quantities cited above. The first one consisted of a 2.14 m (7 feet)

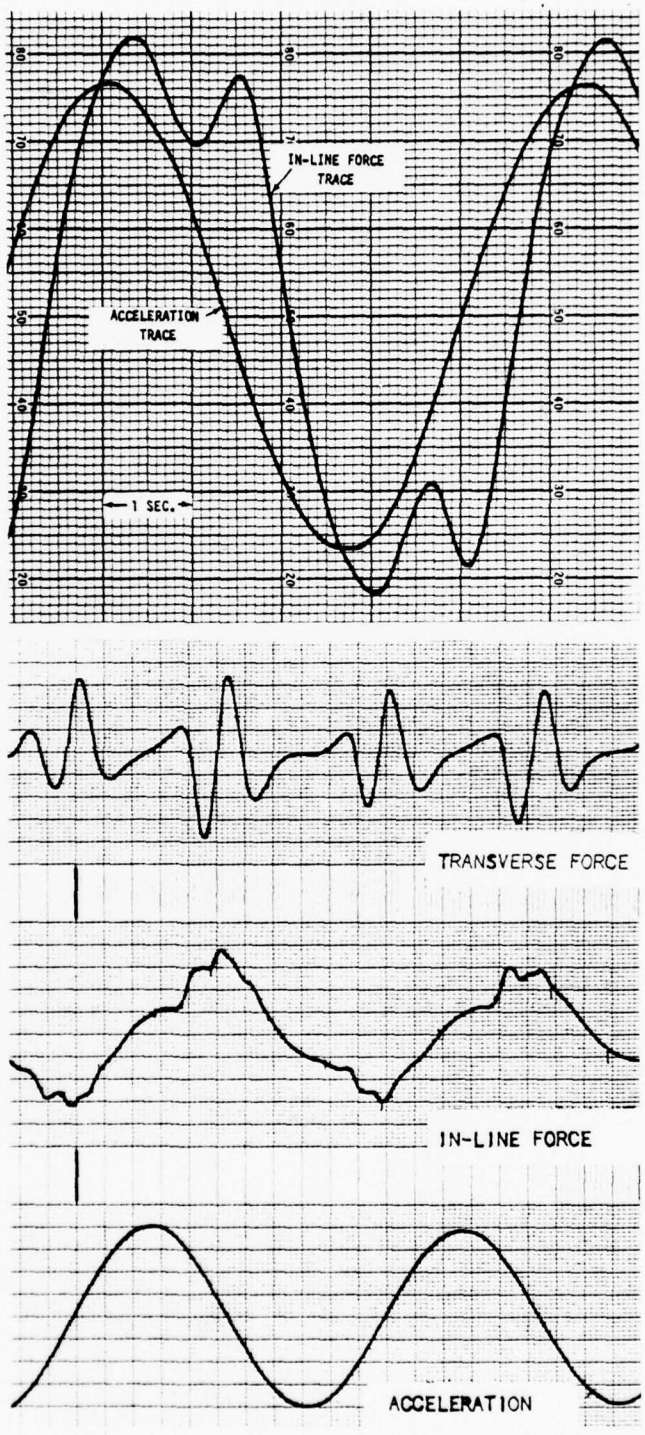

Fig. 4 Acceleration and in-line force traces

long platinum wire stretched vertically in one leg of the tunnel. The output of the capacitance-wire bridge was connected to an eight channel amplifier-recorder system. The response of the wire was found to be perfectly linear within the range of oscillations encountered. The wire was capable of yielding a measurable signal for changes in water elevation as small as 0.8 mm (1/32 inches). Such a sensitivity was not, however, always desirable for the instabilities on the water surface gave rise to small oscillations in the analog records. The effect of such instabilities was practically eliminated by placing the wire along the axis of 30 cm (1 foot) diameter and 213 cm (7 feet) long thin plastic pipe. Be that as it may, the use of this wire was rendered unnecessary due to the use of a more reliable method.

The second method consisted of the measurement of the instantaneous acceleration by means of a differential-pressure transducer connected to two pressure taps placed horizontally 61 cm (2 feet) apart and 91.5 cm (3 feet) to one side of the test section. The output of the transducer was again connected to the eight channel recorder. The instantaneous acceleration was then calculated from $\Delta p = \rho s(dU/dt)$ where Δp is the differential pressure; s is the distance between the pressure taps; and dU/dt is the instantaneous acceleration of the fluid. The effect of the pressure drop due to the viscous forces over the distance s was calculated to be negligible.

The third method again consisted of the measurement of the differential pressure between two pressure taps. The two taps were placed symmetrically on the two vertical legs of the tunnel at an elevation 127.0 cm (50 inches), (see figure 5) below the mean water level, i.e., H = 38 in. Applying Bernoulli's equation for unsteady flow between

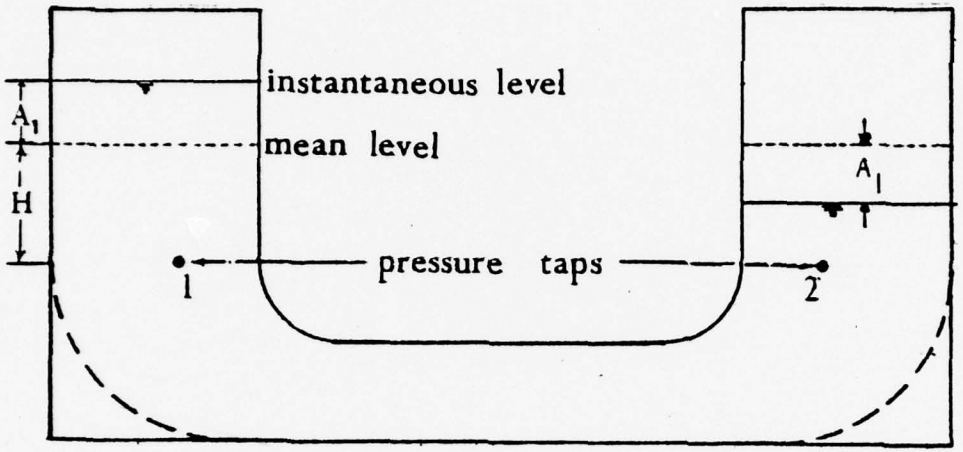

Fig. 5 Position of the Pressure Taps

each pressure tap and the instantaneous level of water, it is easy to show that twice the amplitude of the free surface oscillation (virtual amplitude) is given by

$$A = 2A_1 = \frac{\Delta p/\gamma}{1 - \frac{1}{g}\left(\frac{2\pi}{T}\right)^2 H} \qquad (10)$$

in which g and T are constant and H is kept constant. Thus the signal of this transducer yielded the virtual amplitude or the maximum velocity in each cycle. It was entirely free from noise or small free surface effect. The transducer was calibrated and its linearity checked before each series of experiments.

In addition to all of the methods of measurement described above, the velocity at the test section was directly measured with an MMI, Model 511, Magnetic Velocity Meter, manufactured by "Marsh-McBirney Inc." Suffice it to say that all four methods gave nearly identical results and yielded the amplitude, velocity, or acceleration, to an accuracy of about two percent relative to each other. These comparisons, as well as the perfectly sinusoidal and noise-free character of all pressure and force traces, speak for the suitability of the unique test facility used in this study.

IV. DISCUSSION OF RESULTS

A. BLOCKAGE AND LENGTH-TO-DIAMETER EFFECTS

Attempts to achieve as high a Reynolds number as possible in conducting wind-tunnel or water-tunnel experiments invariably give rise to wall-interference effects. There are several blockage correction formulas for steady flows which might be used so that the wall interference effects might be minimized. Unfortunately none of these formulas could be used in the present study for no one has demonstrated that the blockage effects in oscillatory flows are identical to those experienced in steady flows.

The blockage ratio D/w, where D is the diameter of the cylinder and w the width or height of the test section, and the length- or span-to-diameter ratio, L/D, for the cylinders used in the present study are tabulated below [w = 91.44 cm (3 feet), L = 90.885 cm (2.9818 feet)].

TABLE I

D	D/w	L/D
17.780 cm (7.000 inches)	0.19	5.14
16.447 cm (6.475 inches)	0.18	5.52
15.177 cm (5.975 inches)	0.17	5.99
12.674 cm (4.990 inches)	0.14	7.17
10.103 cm (3.978 inches)	0.11	8.99
7.544 cm (2.970 inches)	0.082	12.05
6.349 cm (2.4996 inches)	0.069	14.31
5.057 cm (1.991 inches)	0.055	17.97

In Achenbach [4] and some of the experiments of Fage and Falkner [9] the blockage ratios were 0.166 and 0.185 respectively. The length-to-diameter ratio in Fage and Warsap's [3] experiments was 20.2 or 7.88, depending on the diameter of the two cylinders they used, as compared to 3.33 in the experiments of Achenbach. Evidently, the formulas used for steady flow correction effects cannot be applied to oscillating flows and there is not a unique blockage correction for the entire period of the harmonic flow. This is evident from the fact that within a given cycle of oscillation the fluid undergoes varying accelerations and velocities and the wake width, momentum deficiency, and the wake pressure change accordingly. Thus, a blockage correction made for the instant of maximum velocity is not applicable to the instant at which the maximum acceleration occurs. In view of the fact that there are no previous investigations, a series of experiments had to be conducted to determine the role of blockage in the flow under consideration. For this purpose a differential pressure transducer was connected to two pressure taps on the same side of the tunnel wall. One of the taps was placed on the wall directly above the axis of the test cylinder. The other tap was placed 76 cm (29.92 inches) to one side of the first tap along a line parallel to the flow. A series of experiments was carried out with the 16.447 cm (6.475 inches) cylinder. The differential pressure was recorded and compared with the differential pressure obtained from the acceleration transducer. Furthermore, to simplify the comparison both transducers were calibrated so as to render exactly the same output under identical calibration loads. The results have shown that the two differential pressures were nearly identical and that they were certainly

within three percent of each other. Often the two traces of two transducers were indistinguishably coincident. This somewhat surprising result is a clear indication of the fact that the blockage effect in harmonic flows is negligible at least for D/w ratios less than about 0.20. Although no special attempt was made to interpret the lack of blockage effect in such flows, it is believed that the presence of vortices on both sides of the cylinder together with the high periods of acceleration and velocity renders the flow relatively more uniform at short distances away from the cylinder in the test section. Therefore, for the reasons cited above no blockage-effect corrections were applied to the data presented here. It might be of interest to note that had the flow been assumed uniform and had the maximum velocity for the largest cylinder and the Reynolds number been used to calculate a blockage effect correction through the use of one of the existing formulas, one would have found that such a correction would have amounted to about six percent.

B. IN-LINE FORCE DATA

The drag and the inertia coefficients, obtained through the use of equations (2) and (3) and the computer program presented in Appendix A, have been plotted for each cylinder and relative roughness as a function of K for various constant values of β. As cited earlier, experiments were ordinarily carried out at three representative temperatures or, in other words, at three constant values of β. Experiments at each temperature were repeated at least twice. Representative drag and inertia coefficient plots for D = 10.103 cm (3.978 inches), k/D = 1/400, β = 3130, β = 2350, and β = 1770 are shown in figures (6) and (7) as a

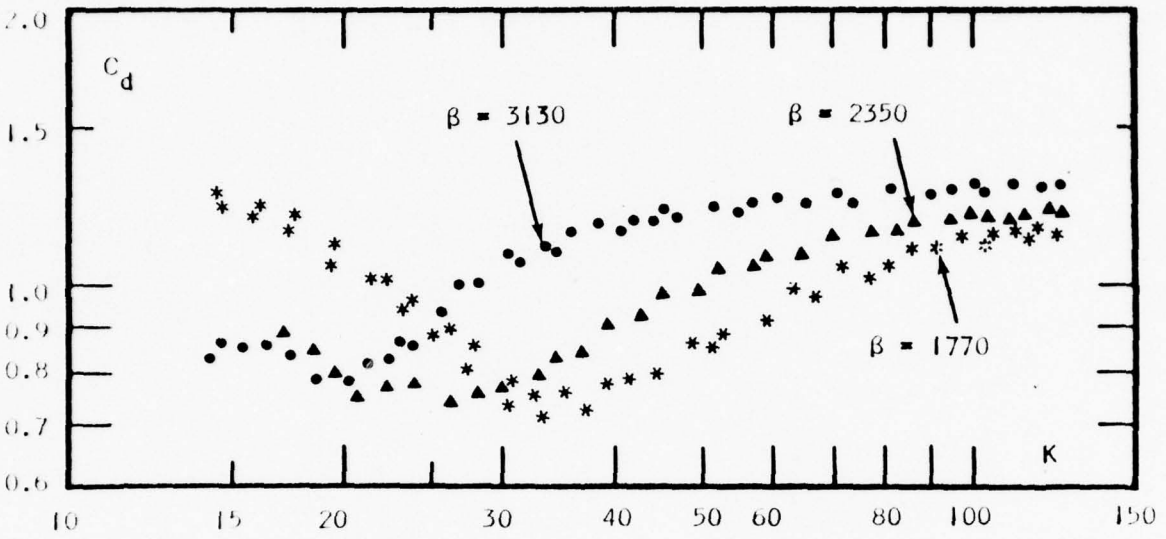

Fig. 6 C_d versus K plot for 4 inch cylinder (k/D = 1/400)

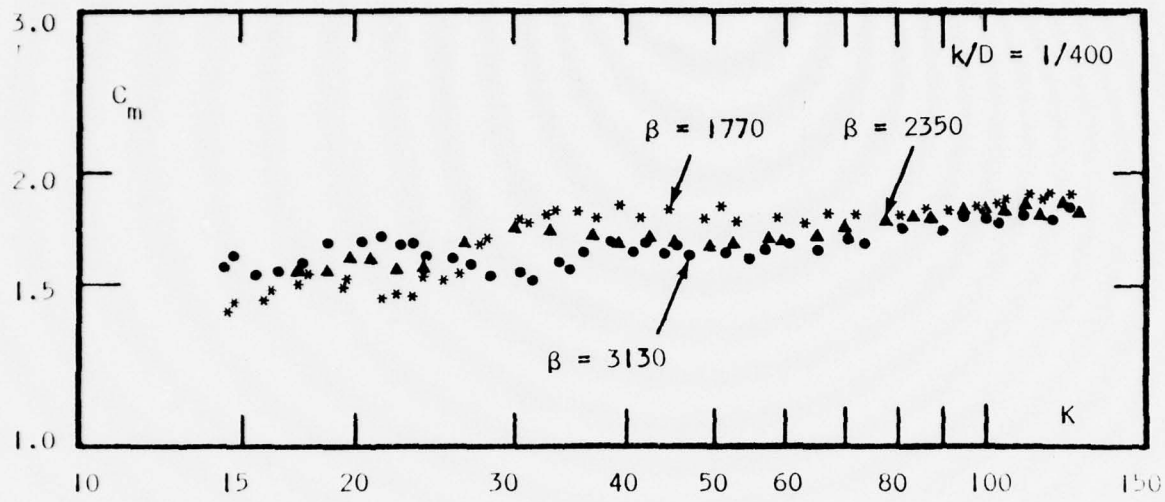

Fig. 7 C_m versus K plot for 4 inch cylinder (k/D = 1/400)

function of the Keulegan-Carpenter number. For this particular series of tests, K ranged from about 15 to 125, and the Reynolds number from about 26,000 to 400,000. Each plot for each β shows the results from two different runs. Evidently, the experiments are perfectly repeatable, and the deviation from a mean line drawn through the data for a constant β is less than five percent. It is also evident from these plots that both the drag and the inertia coefficients undergo rather important changes in the range of K values around 20. For larger values of K both C_d and C_m cease to vary significantly with the Keulegan-Carpenter number.

Even though the frequency parameter β is quite powerful in plotting the data, interpreting the results, and giving a measure of the thickness of the laminar boundary layer over a cylinder (the boundary layer thickness δ is inversely proportional to the square root of β), it is customary in the practical engineering world to express the force-transfer coefficients in terms of the Reynolds number. As described earlier, one can choose a particular value of K and calculate the Reynolds number for a given β simply through the use of $Re = \beta K$.

Such a procedure enables one to express C_d or C_m as a function of the Reynolds number for a given K and k/D. In view of the fact that each coefficient depends on at least three independent parameters (Re, K, k/D), it is not possible to show on two-dimensional plots the variation of either C_d or C_m for all values of Re, K, and k/D. However, this difficulty is alleviated by the fact that the variation of a given force coefficient for a given Re and k/D is not very strong from one K to another. Thus it has been decided to choose five representative K values, namely K = 20, 30, 40, 60, and 100, to present the variation of C_d and C_m with Re.

Figures (8) through (12) and figures (13) through (17) show C_d and C_m respectively for the five values of K as a function of the Reynolds number. Each curve on each plot corresponds to a particular relative roughness. Also shown on each figure is the corresponding drag or inertia coefficient for the smooth cylinder at the corresponding K value.

The k/D = constant curves on each C_d plot are quite similar to those found for steady flow about rough cylinders [3,4]. For a given relative roughness, the drag coefficient does not significantly differ from its smooth cylinder value at very low Reynolds numbers. As the Reynolds number increases, C_d for the rough cylinder decreases rapidly, goes through the region of drag crisis at a Reynolds number considerably lower than that for the smooth cylinder and then rises sharply to a nearly constant transcritical value. The larger the relative roughness the larger is the magnitude of the minimum C_d and the smaller is the Reynolds number at which that minimum occurs. However, there appears to be a minimum Reynolds number below which the results for rough cylinders do not significantly differ from those corresponding to smooth cylinders. In other words, the Reynolds number must be sufficiently high for the roughness to play a role on the drag and flow characteristics of the cylinder.

The figures for the drag coefficient also exhibit a few other interesting features. First, even a relative roughness as small as 1/800 can give rise to transcritical drag coefficients which are considerably higher than those for the smooth cylinder. Secondly, the asymptotic values of the drag coefficient for roughened cylinders (e.g., k/D = 1/100), within the range of Reynolds numbers encountered, can reach values which are considerably higher than those obtained with steady flows over

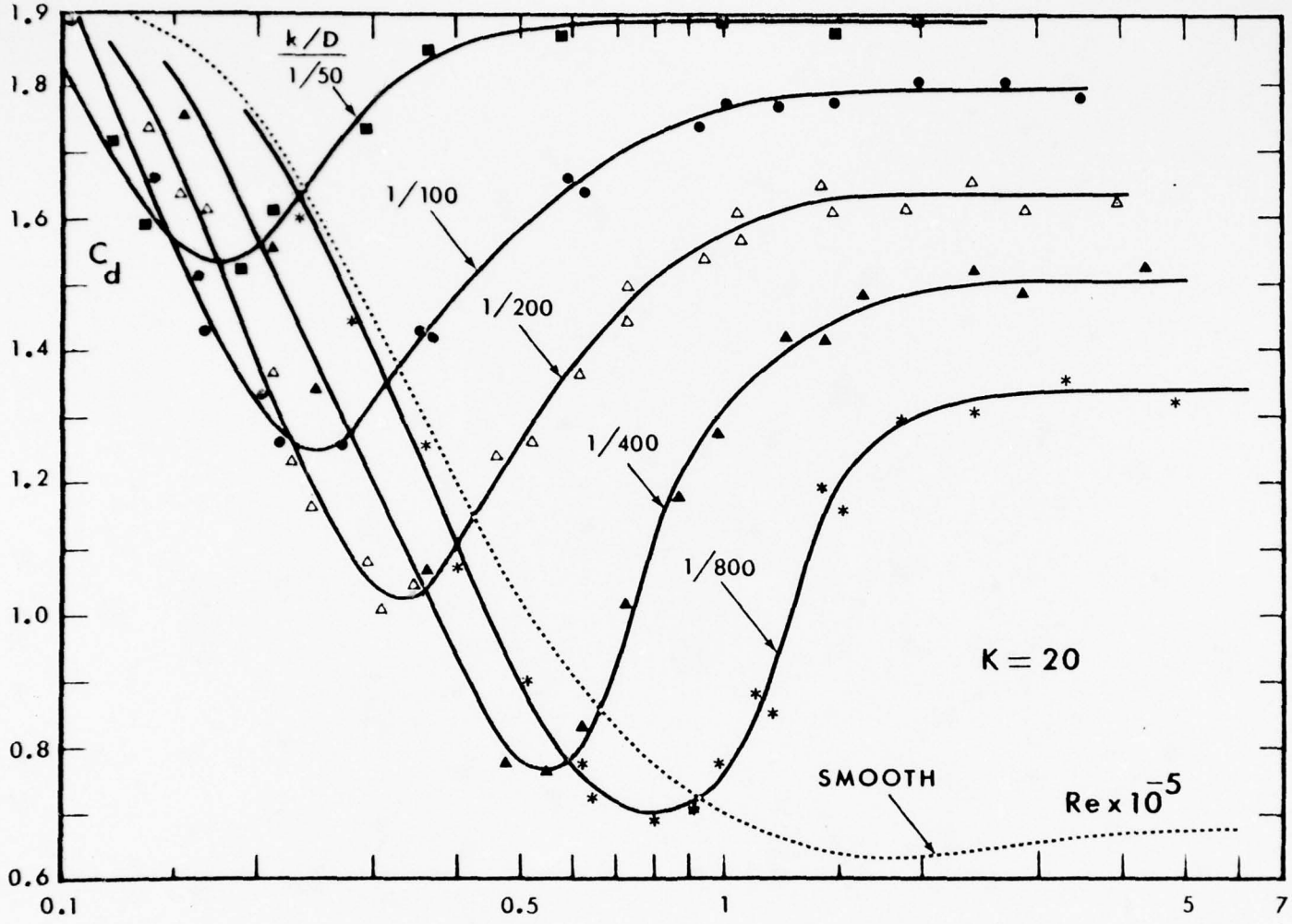

Fig. 8 C_d versus Re for K = 20

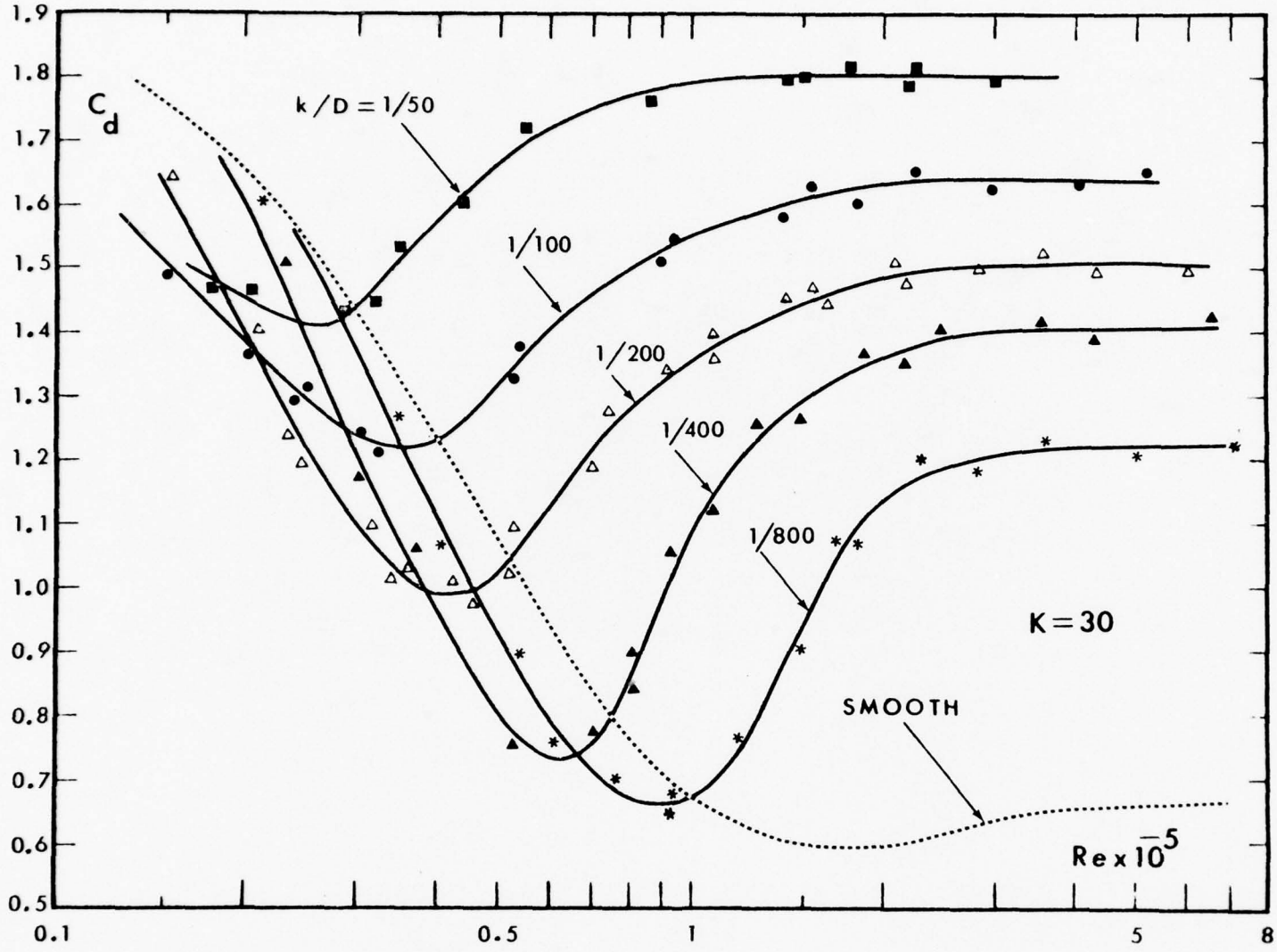

Fig. 9 C_d versus Re for K = 30.

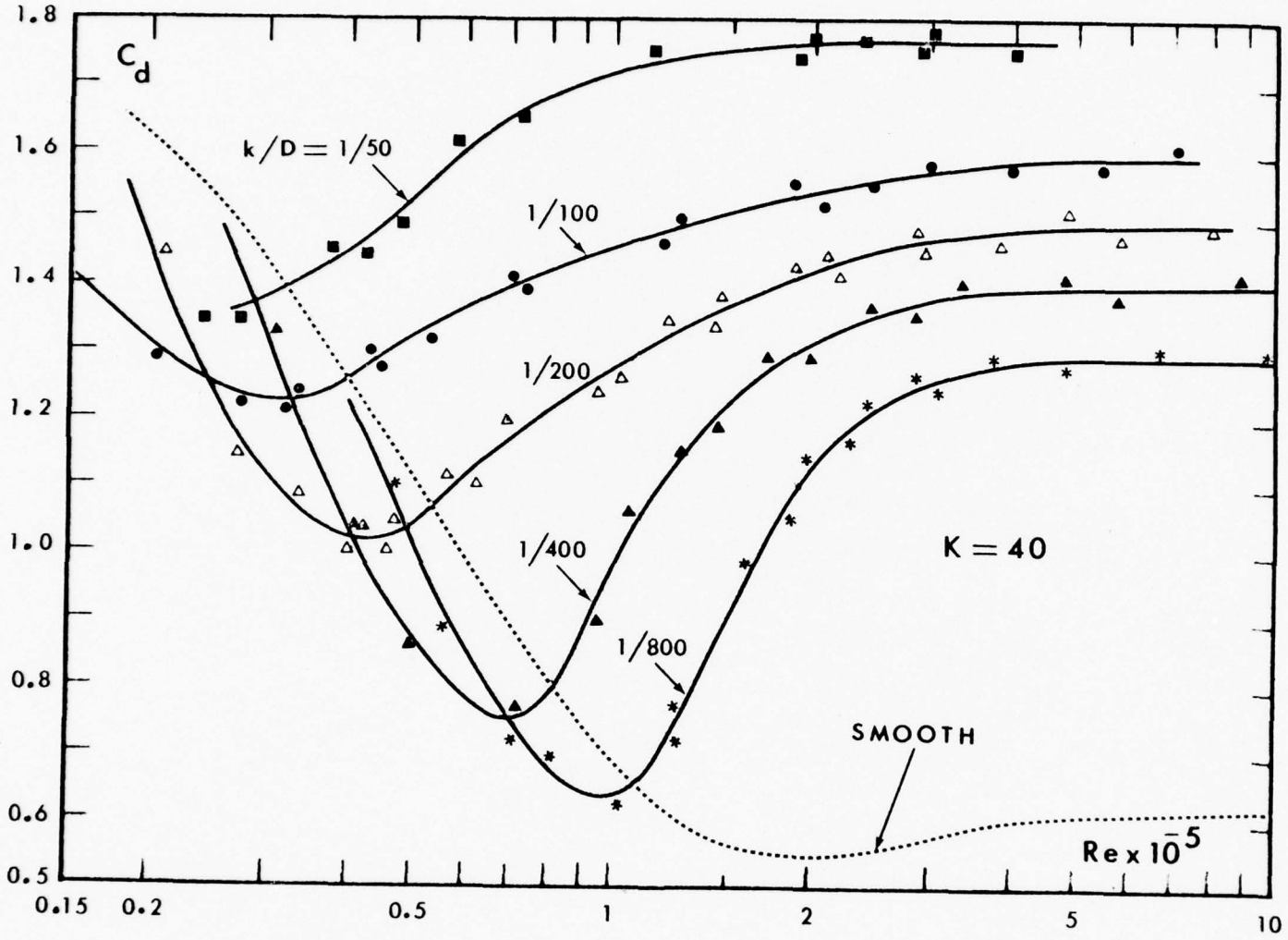

Fig. 10 C_d versus Re for K = 40.

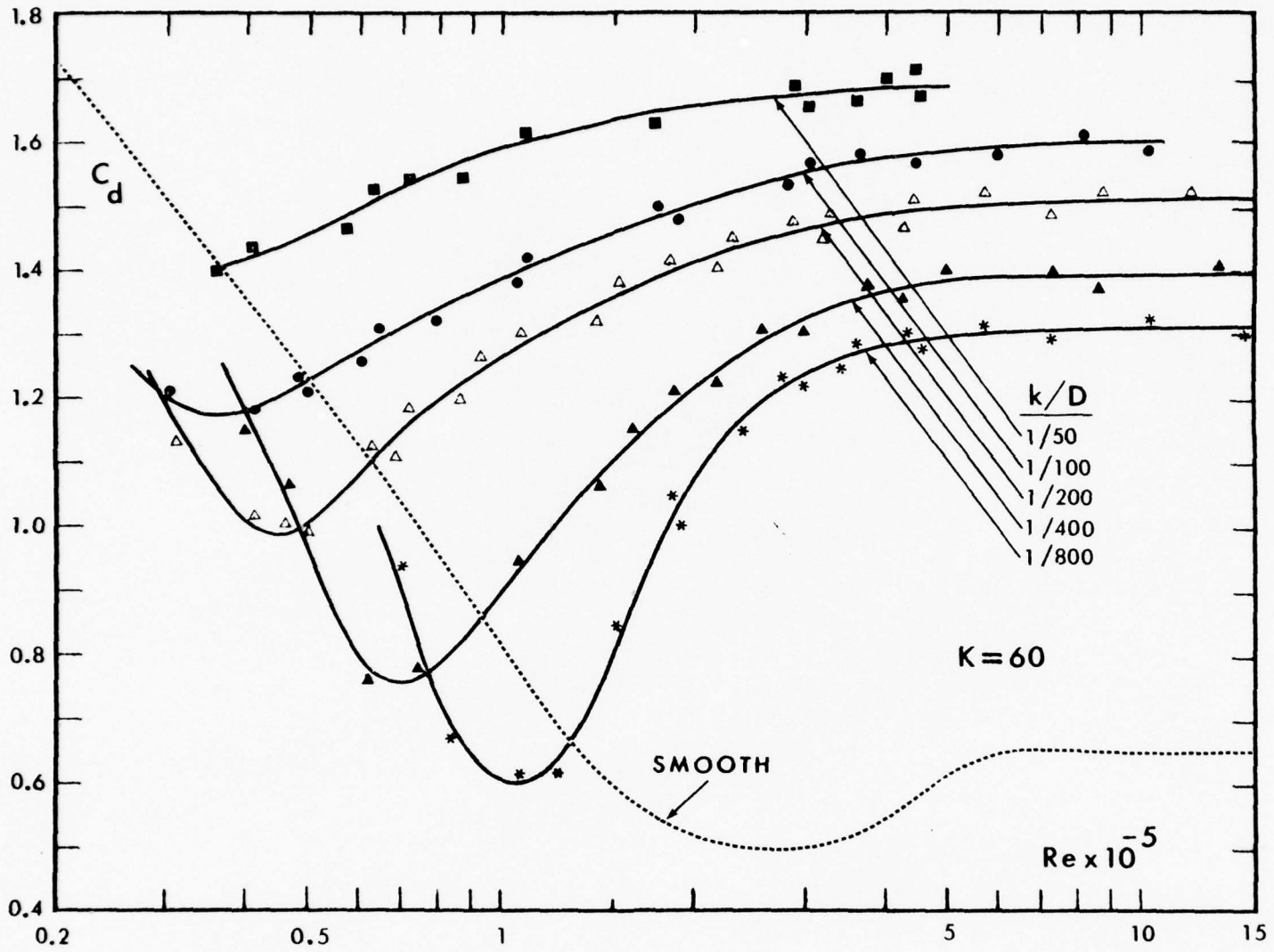

Fig. 11 C_d versus Re for K = 60.

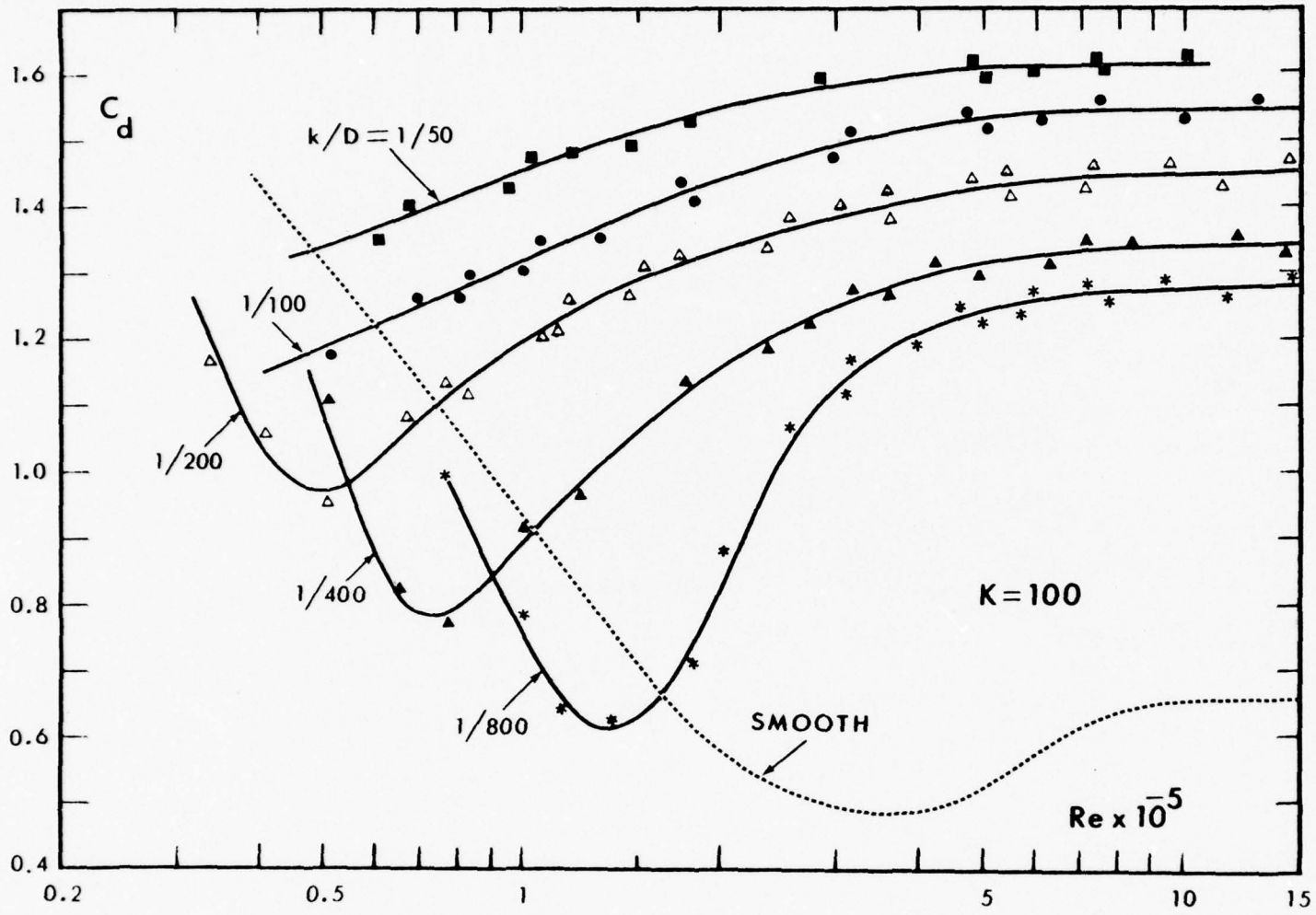

Fig. 12 C_d versus Re for K = 100.

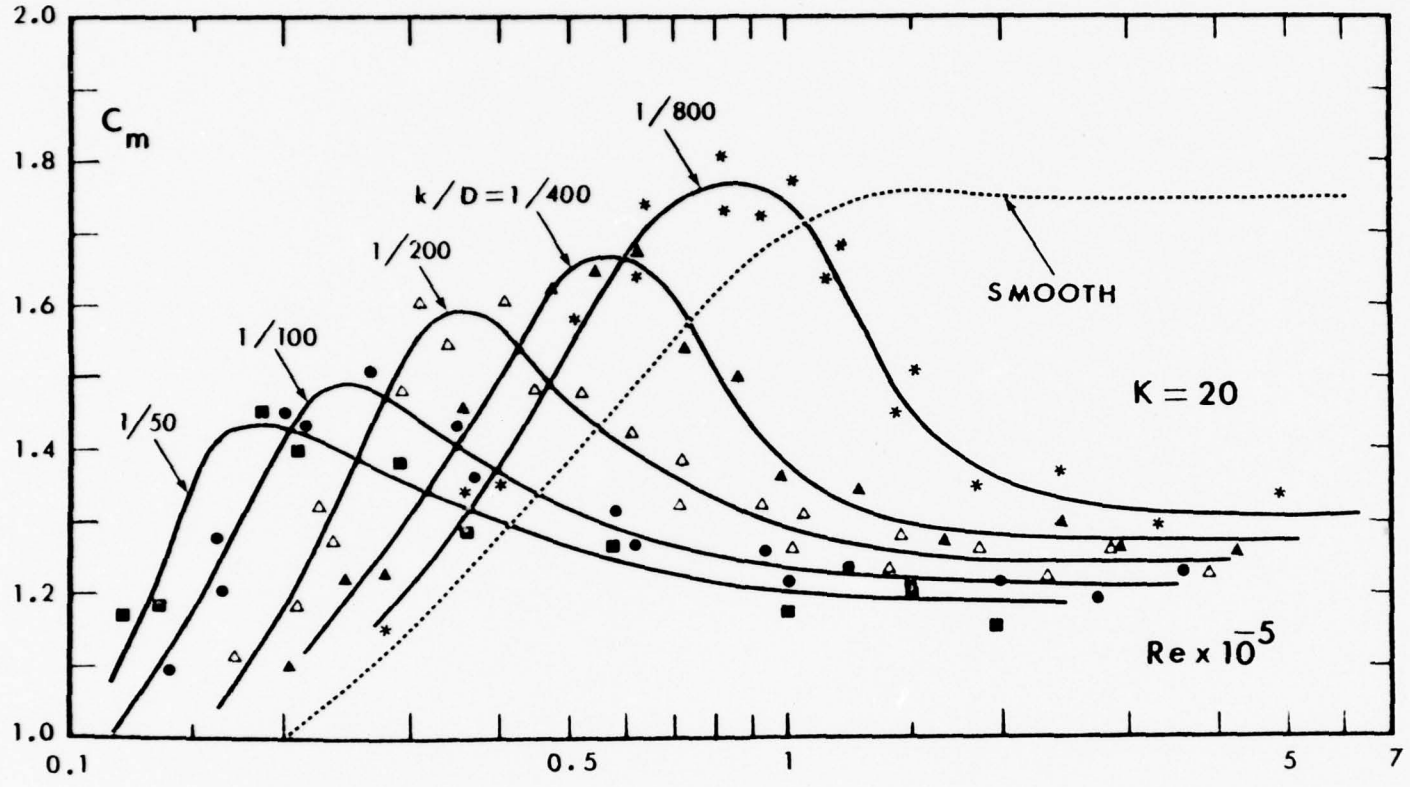

Fig. 13 C_m versus Re for K = 20.

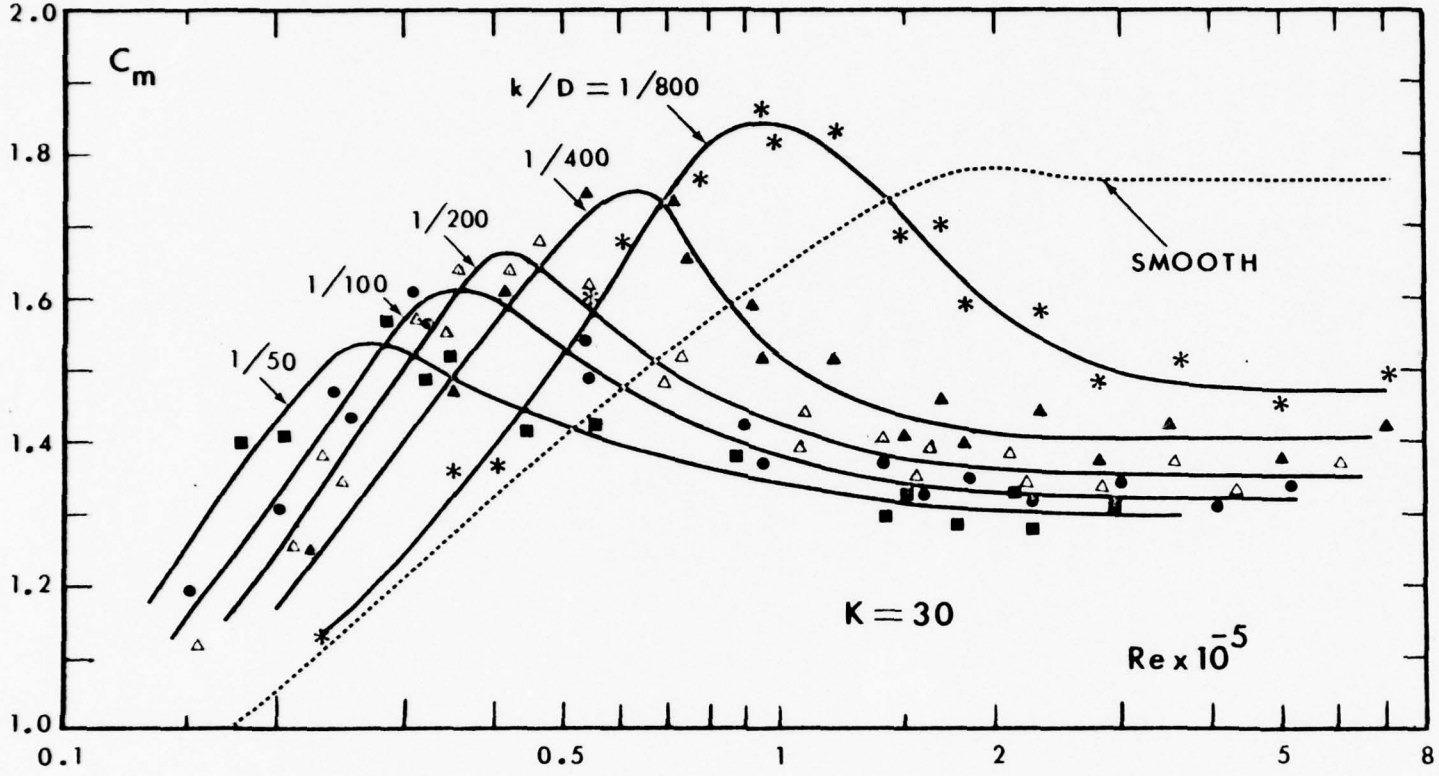

Fig. 14 C_m versus Re for K = 30.

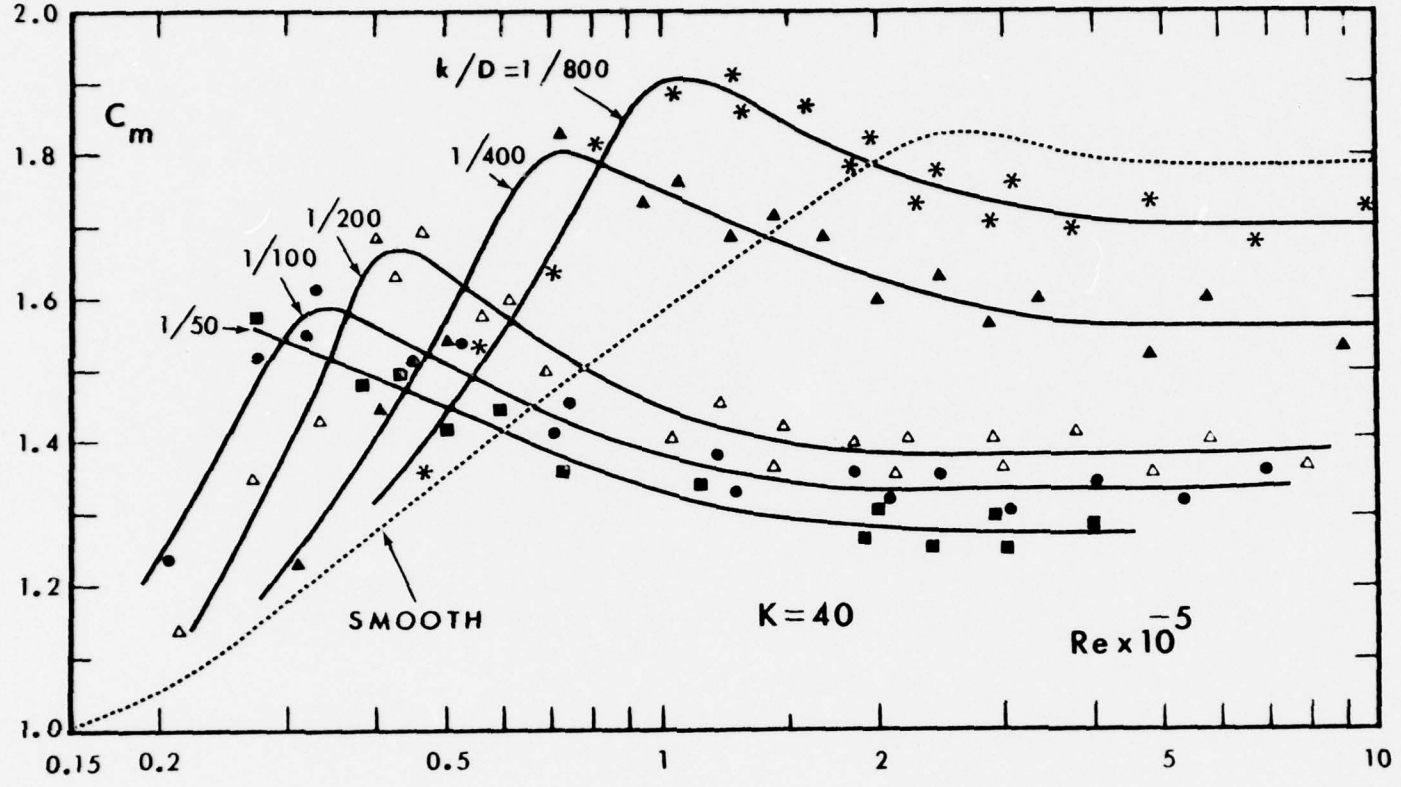

Fig. 15 C_m versus Re for K = 40.

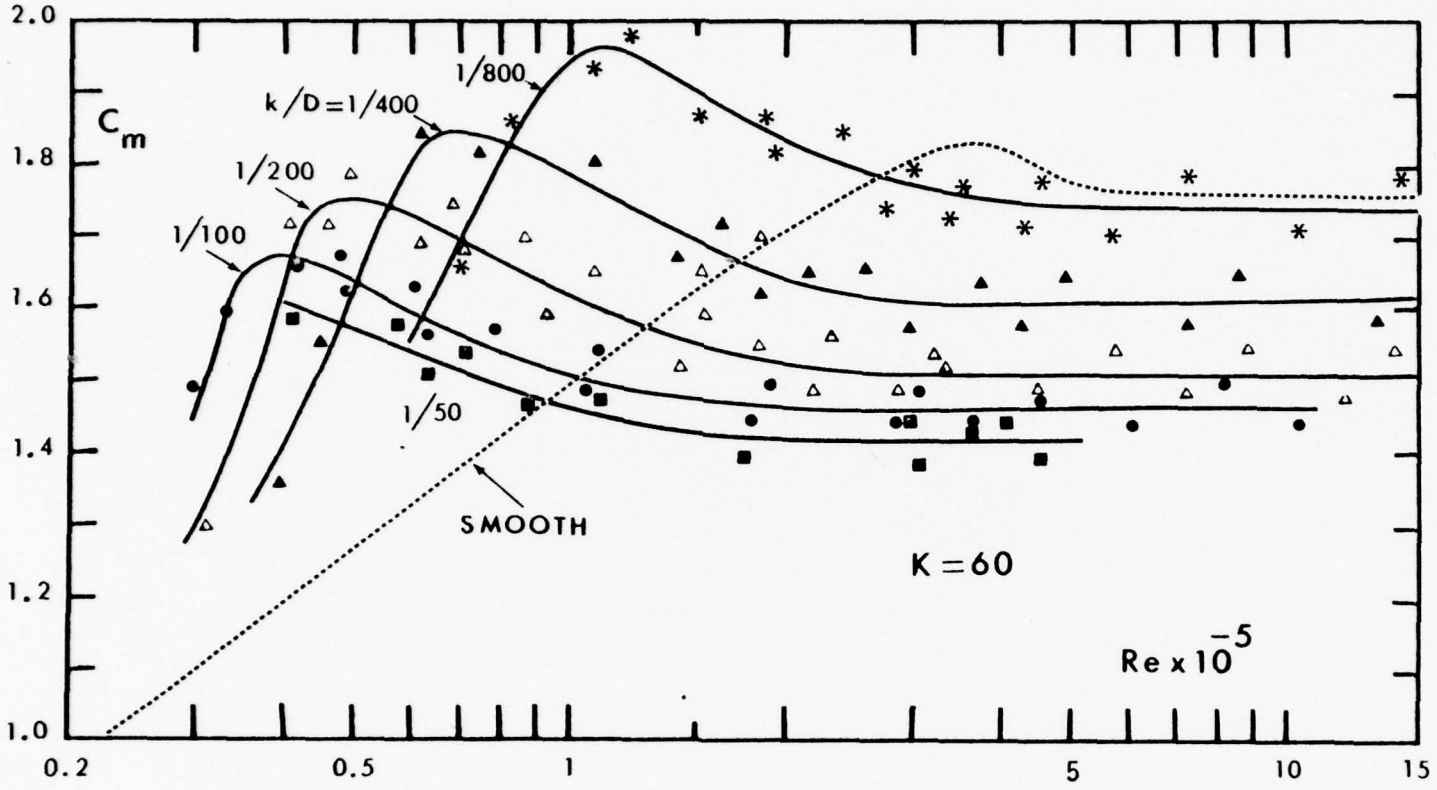

Fig. 16 C_m versus Re for K = 60.

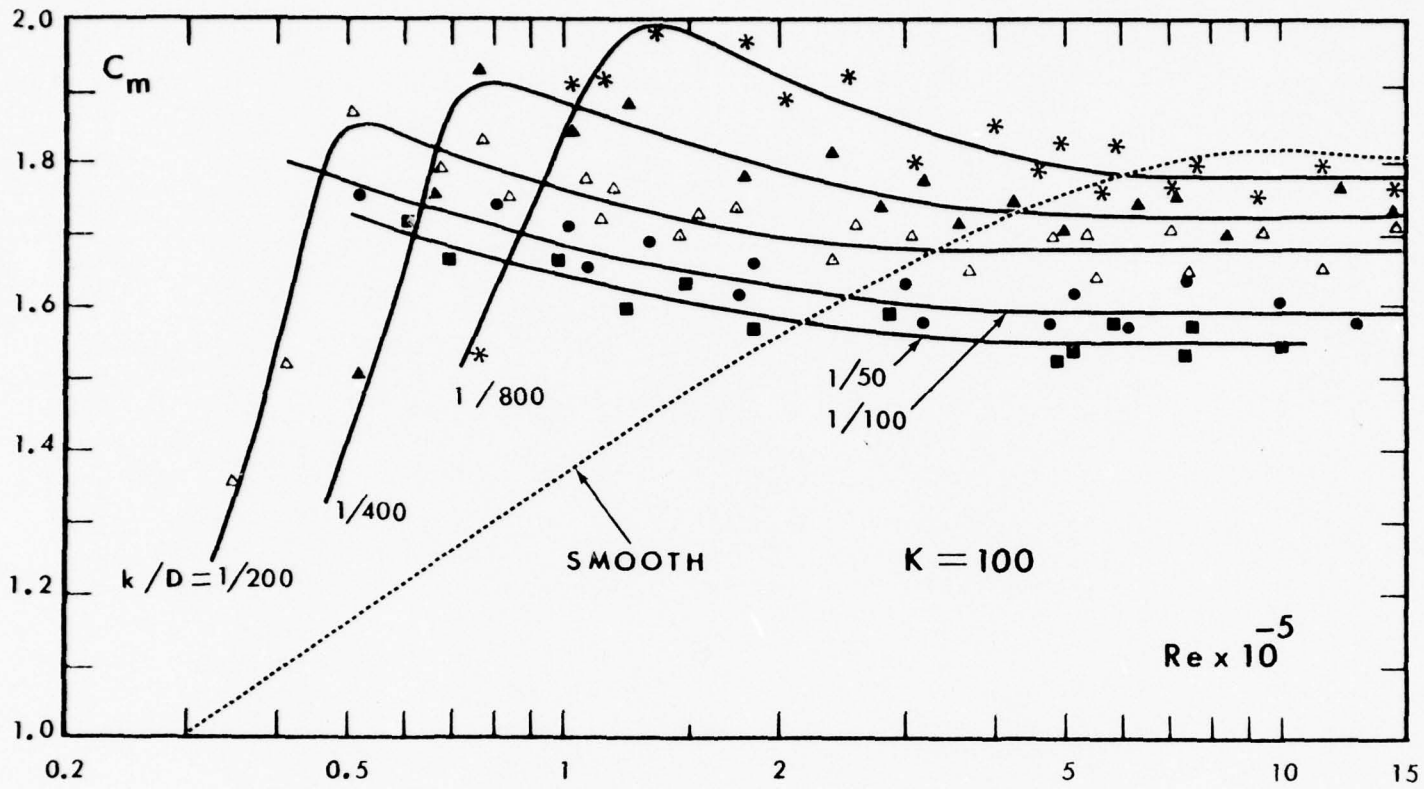

Fig. 17 C_m versus Re for K = 100.

cylinders of similar roughness ratios. In other words, it is not safe to assume that the transcritical drag coefficient in harmonic flows will be identical to those found in steady flows and will not exceed a value of about unity. On the basis of the present results it may be said that such a conjecture is not accurate even for K values as large as 100 (corresponding to a wave height-to-diameter ratio of about 30). It is therefore important to remember that the effect of roughness depends not only on the relative size of the roughness element but also on the characteristics of the ambient flow as well as on the body about which this flow takes place. The characteristics of the ambient flow determine to a large extent the state of the flow (subcritical, critical, and transcritical) during a given cycle of oscillation. The geometry of the body dictates, together with the flow, the variation with time of the separation points. It is therefore not easy to draw a parallel between the behavior of steady flow and that of harmonic flow over a smooth and rough cylinder. In fact, the steady as well as the oscillating flow results for rough cylinders show that, in either case, the transcritical drag coefficient nearly returns to its subcritical values.

The inertia coefficient is shown in figures (13) through (17) as a function of the Reynolds number for the five values of K (K = 20, 30, 40, 60, and 100) and five relative roughnesses (k/D = 1/50, 1/100, 1/200, 1/400, and 1/800). Also shown in the figures are the C_m values corresponding to the smooth cylinder case. It is immediately apparent from these figures that for a given relative roughness, C_m rises rapidly to a maximum at a Reynolds number which corresponds to that at which C_d drops to a minimum. In other words, the Reynolds number at which the drag crisis occurs gives rise to the maximum inertia coefficient for a

given relative roughness. At relatively higher Reynolds numbers, C_m decreases somewhat and then attains nearly constant values which are lower than those corresponding to the smooth cylinders. It is also apparent from figures (13) through (17) that the smaller the relative roughness the larger is the maximum inertia coefficient. For relatively smaller roughnesses such as k/D = 1/800, the terminal value of C_m is nearly equal to that of a smooth cylinder.

The behavior of C_m is not entirely unexpected. It has long been noted [6] that whenever there is a rise in the drag coefficient, there also is a decrease in the inertia coefficient.

Before closing the discussion of the drag and inertia coefficients, it is necessary to point out the remarkably consistent behavior of the data points, particularly for C_d. Perhaps it would not have been too surprising had the data been obtained for one relative roughness through the use of only one cylinder. In the present investigation, the use of several cylinders and several temperatures for a given cylinder always provided data for nearly identical k/D, Re and K values. For instance, the C_d and C_m values obtained at a given K, Re, and relative roughness k/D, using a 12.7 cm (5 inch) cylinder at a low temperature (about 55°) corresponds to the C_d and C_m values using a 10.2 cm (4 inch) cylinder at a higher temperature (about 115°). Remembering the fact that not only the actual size of the cylinders but also the size of the sand grains differed in order to obtain the same k/D, and the fact that the experiments were carried out at different temperatures and times, one fully realizes that the correlation of the data and the relatively small scatter are indeed quite remarkable. This is due not only to the repeatability of the tests but also due to the vibration-free operation of the entire tunnel system.

C. APPLICABILITY OF MORISON'S EQUATION

Since its inception, questions have been raised regarding the applicability of Morison's equation to time-dependent flows in general and to wavy flows in particular. It has been known that the equation predicts quite accurately the in-line force for both very small values of K (K smaller than about 10) and for large values of K (K larger than about 20). For intermediate values of K, differences have been observed between the measured and calculated values. These differences have been attributed either to the imprecise measurement of the kinematics of the flow or to the shortcomings of the equation. It is now realized that not only these two factors (namely the heuristic nature of the equation and the difficulty of measuring local velocities and accelerations) but also the three-dimensional nature of the wavy flows and decreased spanwise coherence must be partly responsible for the differences between the measured and calculated forces. In fact, it would have been extremely difficult to draw meaningful conclusions concerning the applicability of Morison's equation through the use of the field data. It is only through the use of carefully conducted two-dimensional harmonic flow experiments that one can ascertain the degree of applicability of Morison's equation.

Figures (18) through (27) show the calculated and measured forces normalized by $0.5\ \rho DLU_m^2$ together with the normalized velocity and the difference between the measured and calculated forces. It is evident that there is often a remarkable correspondence between the measured and predicted forces particularly for K values larger than about 20. This is also true for K smaller than about 10. In the range of K values between 10 and 20, the fractional sheeding of vortices [1] gives rise to additional oscillations in the in-line force. Consequently, the measured and calculated forces do not quite correspond, particularly

near their maximums. The transverse-force-induced oscillations in the in-line force may be taken into consideration by calculating two additional terms in the Fourier series expressing the force, as done by Keulegan and Carpenter [6]. In this manner, one can reduce the difference between the measured and calculated forces in the neighborhood of $K = 15$. This method will not be described here further. Suffice it to note that additional terms have been calculated in the Fourier series and the effect of the corrections brought about by these terms on the prediction of the Morison's equation has been examined. The results have shown that outside the range of $20 < K < 10$, the effect of such corrections is negligible.

It may be said in view of the foregoing and the examination of several hundred other force traces similar to those shown in figures (18) through (27) that Morison's equation predicts the measured force for rough as well as smooth cylinders with remarkable accuracy. It should be kept in mind that the kinematics of the flow field must be known accurately and that there must not be complex three-dimensional flows. The three-dimensional flow effects cannot be simply incorporated into the equation. In fact, what remains to be resolved as one of the most important practical problems of fluid loading on offshore structures is the role played by three-dimensionality and the lack of spanwise coherence. The drag coefficients presented herein obviously represent their maximum possible values for they have resulted from a purely uniform, two-dimensional flow where the instantaneous wake of the cylinder has the highest possible degree of spanwise correlation.

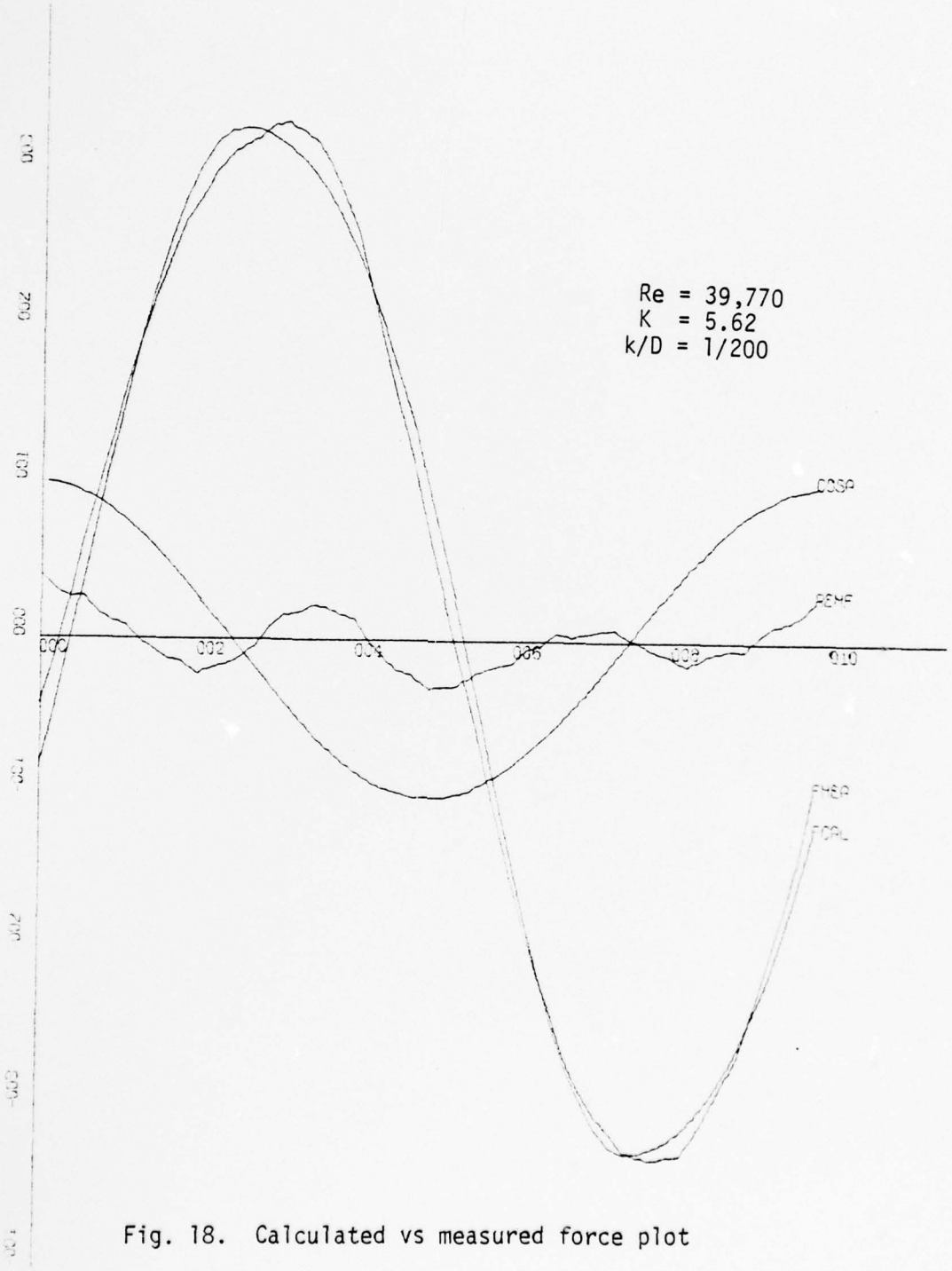

Fig. 18. Calculated vs measured force plot

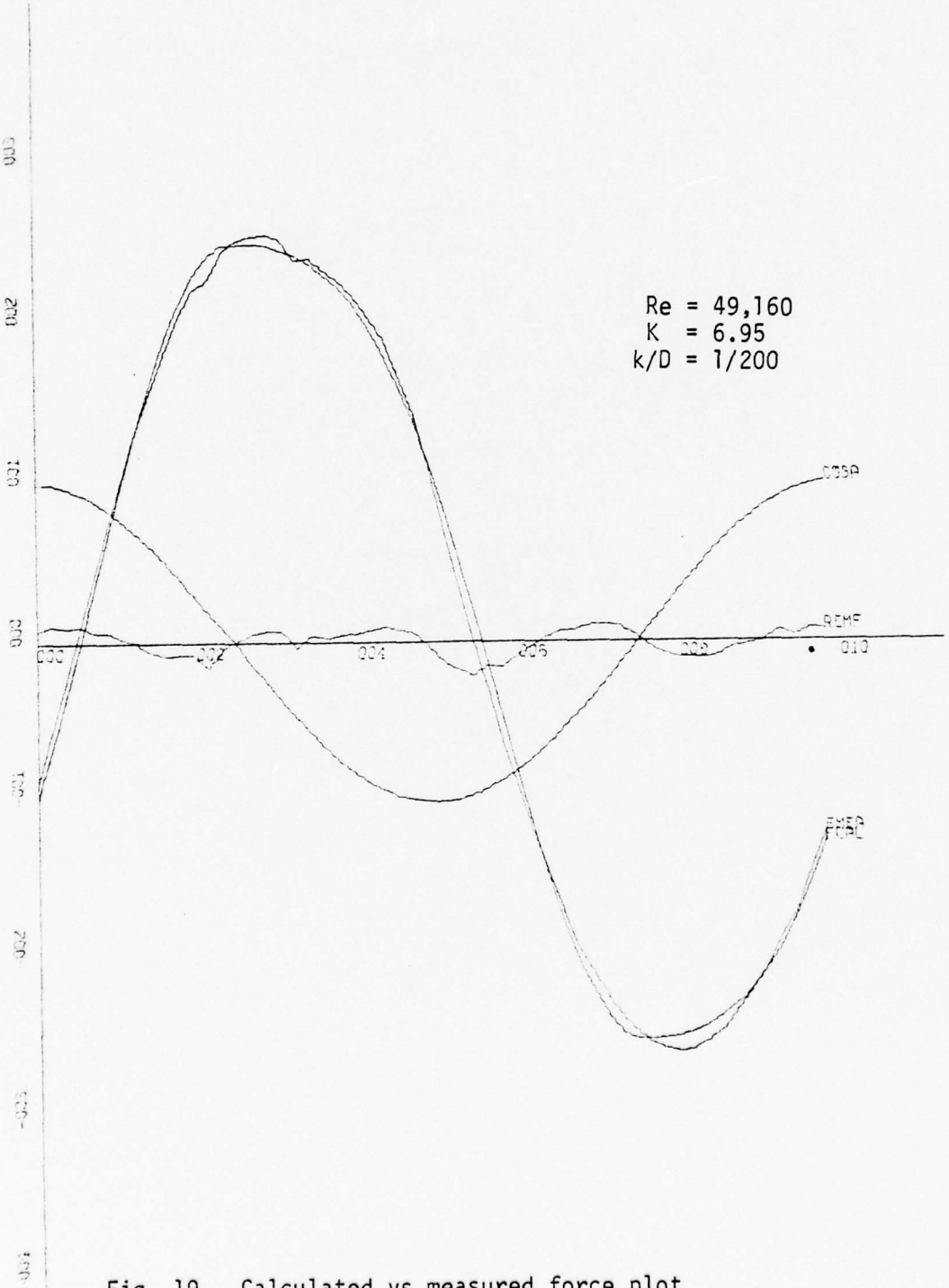

Fig. 19. Calculated vs measured force plot

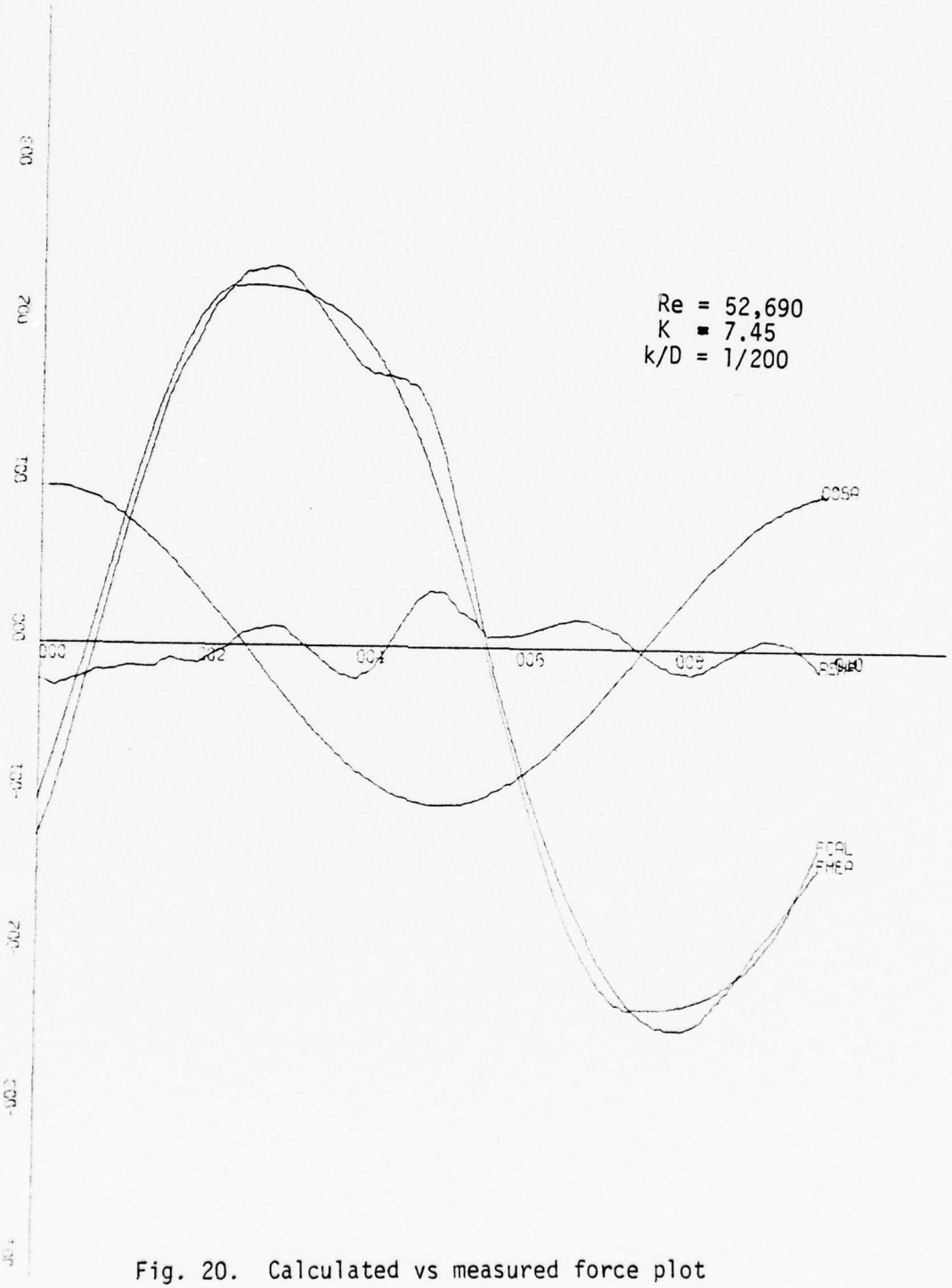

Fig. 20. Calculated vs measured force plot

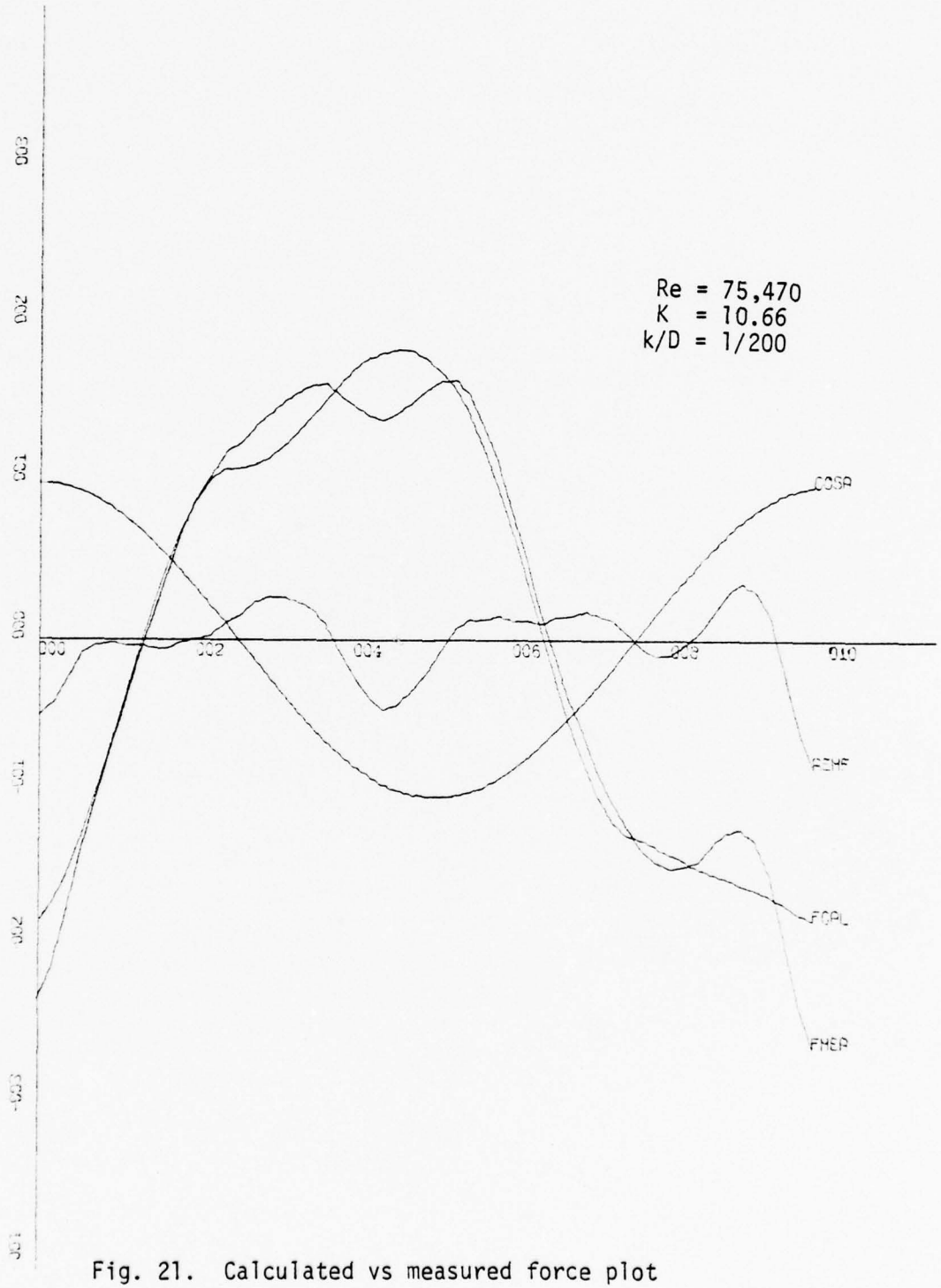

Fig. 21. Calculated vs measured force plot

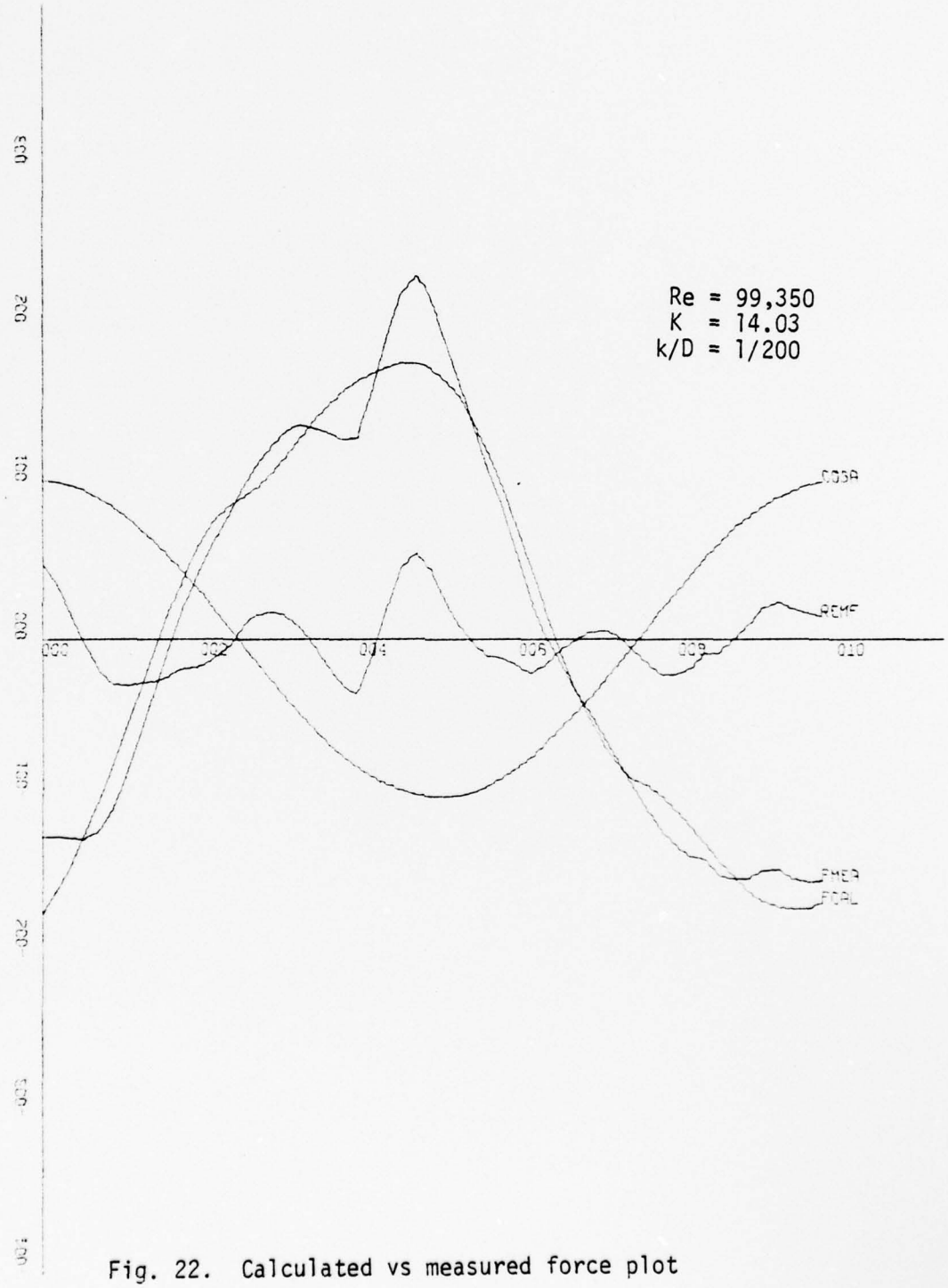

Fig. 22. Calculated vs measured force plot

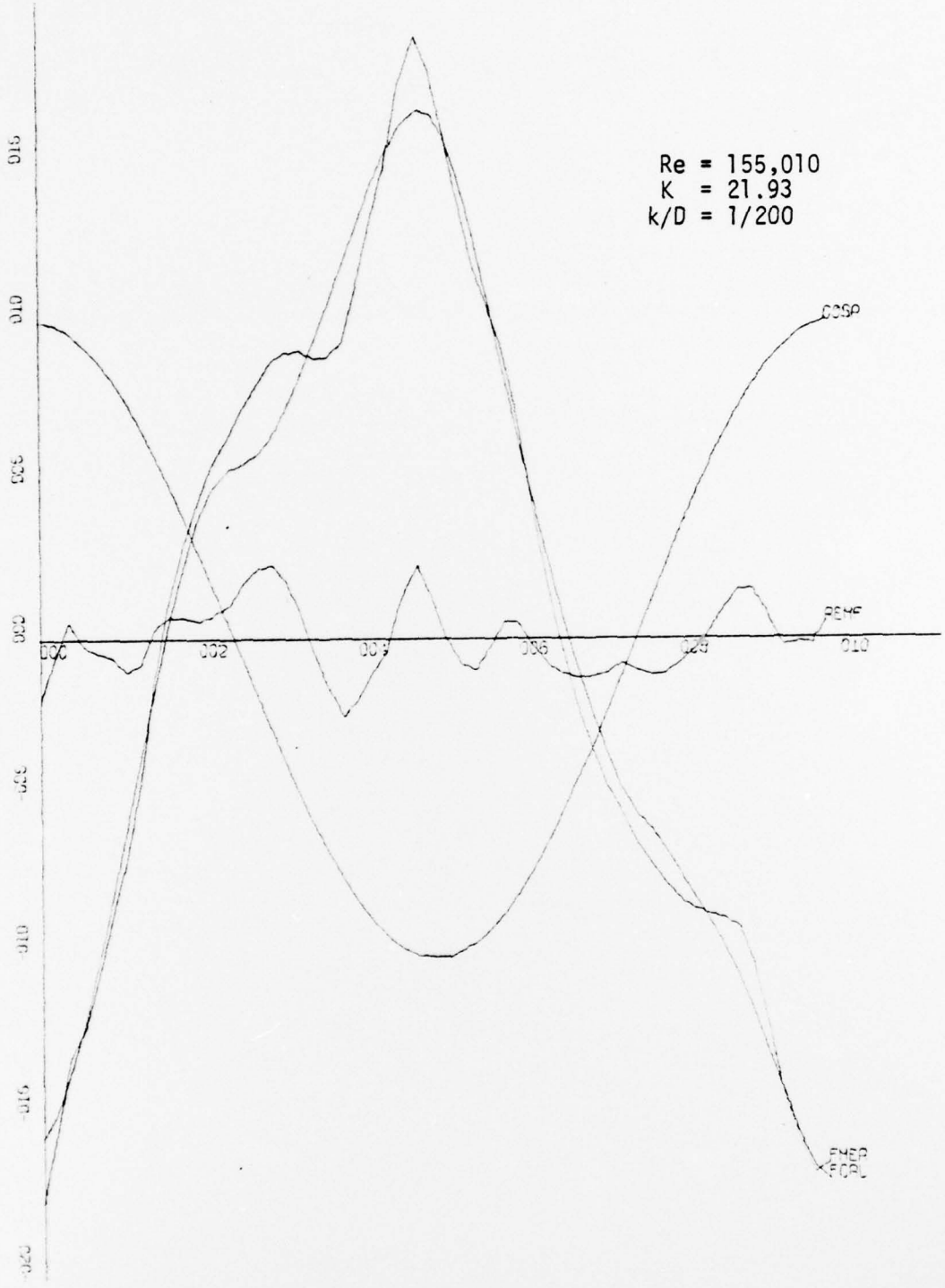

Fig. 23. Calculated vs measured force plot

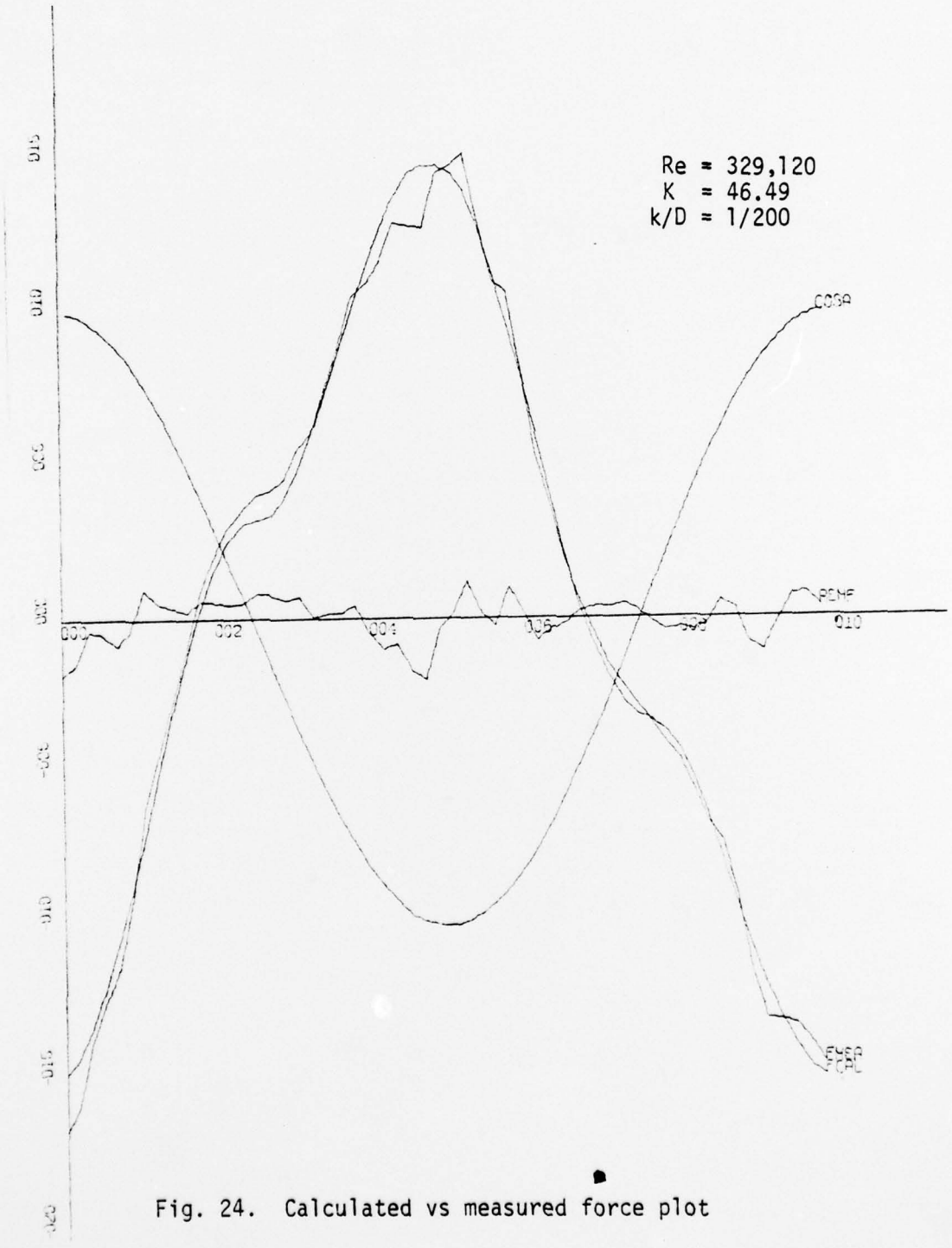

Fig. 24. Calculated vs measured force plot

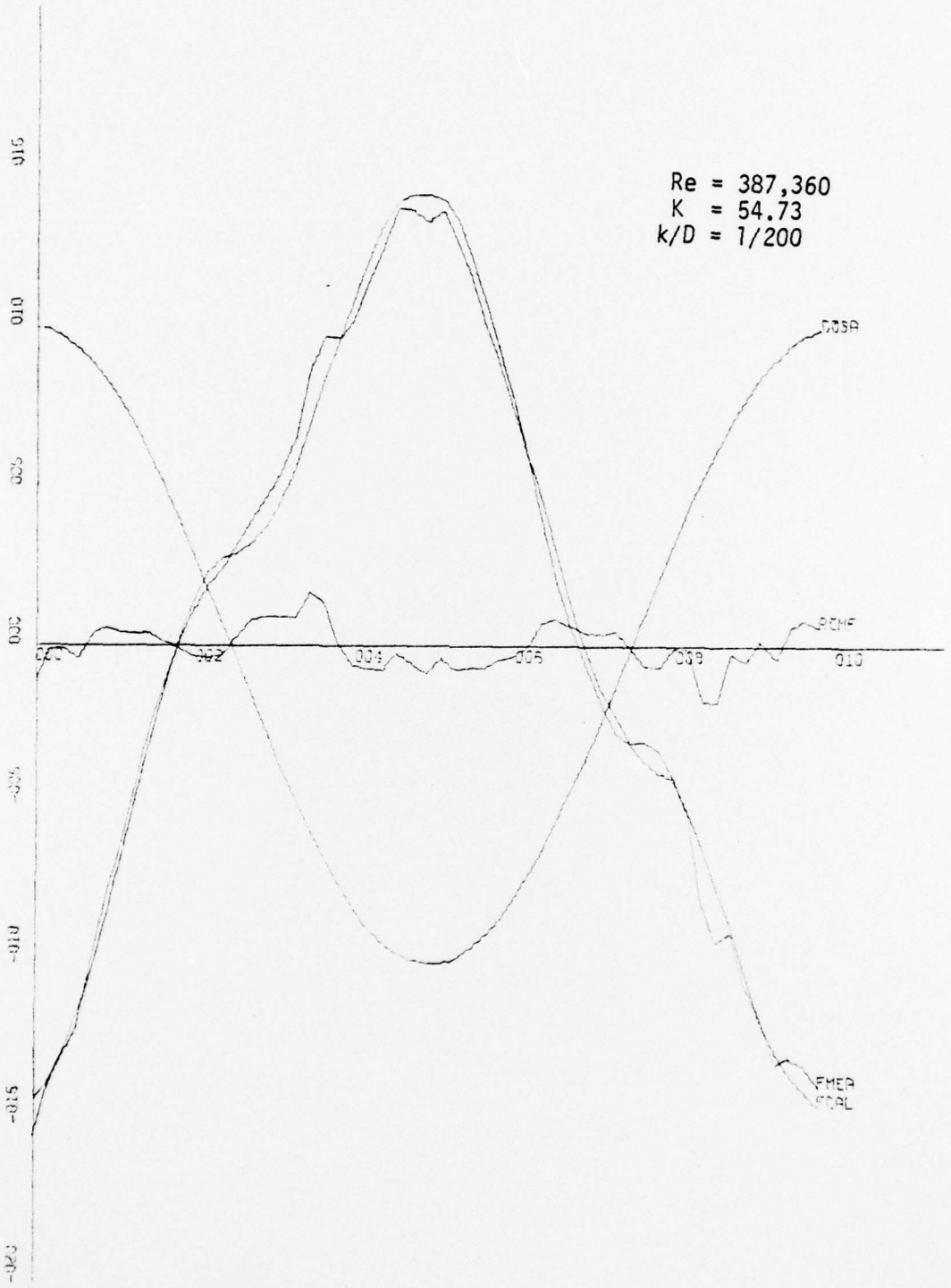

Fig. 25. Calculated vs measured force plot

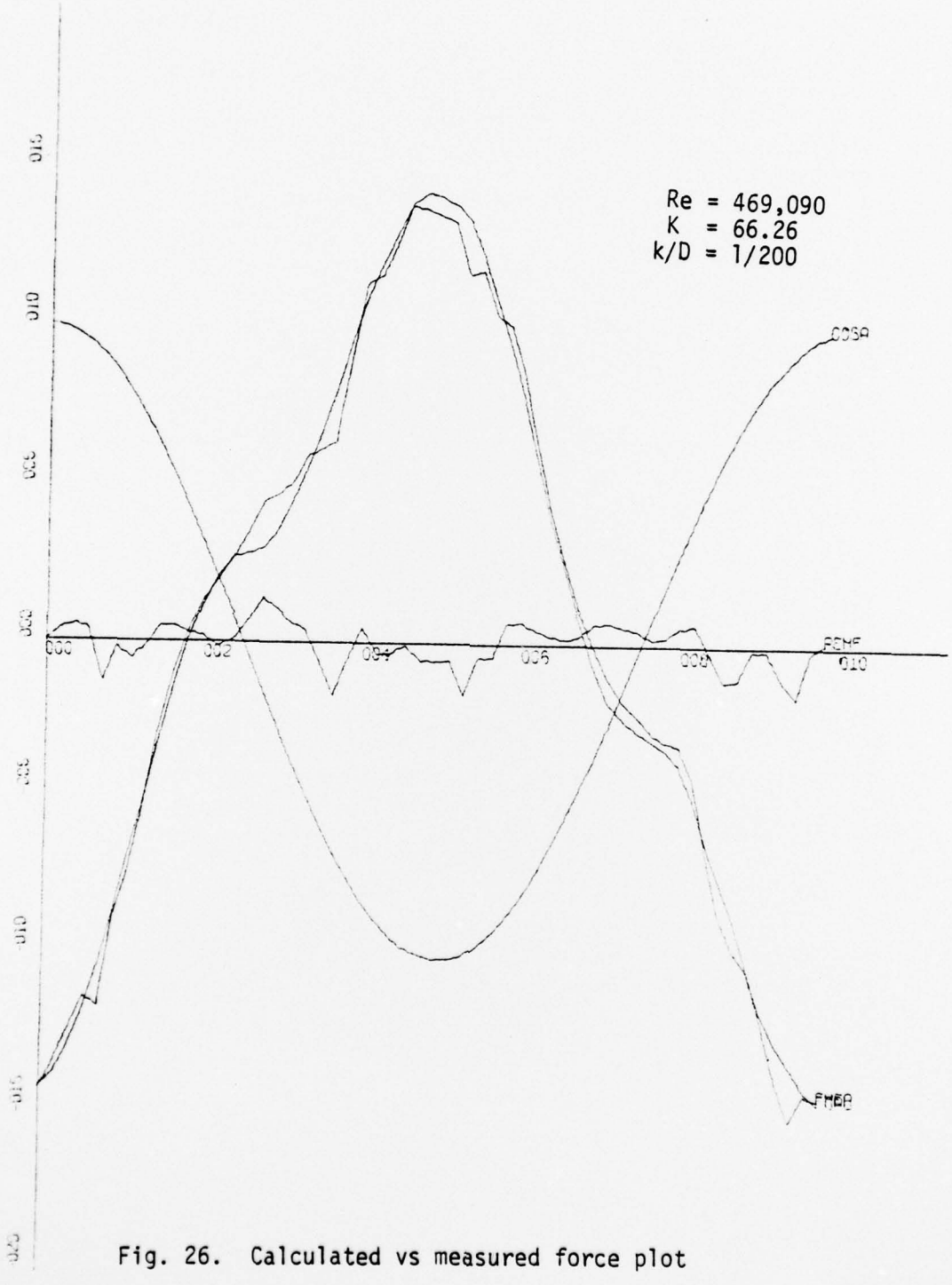

Fig. 26. Calculated vs measured force plot

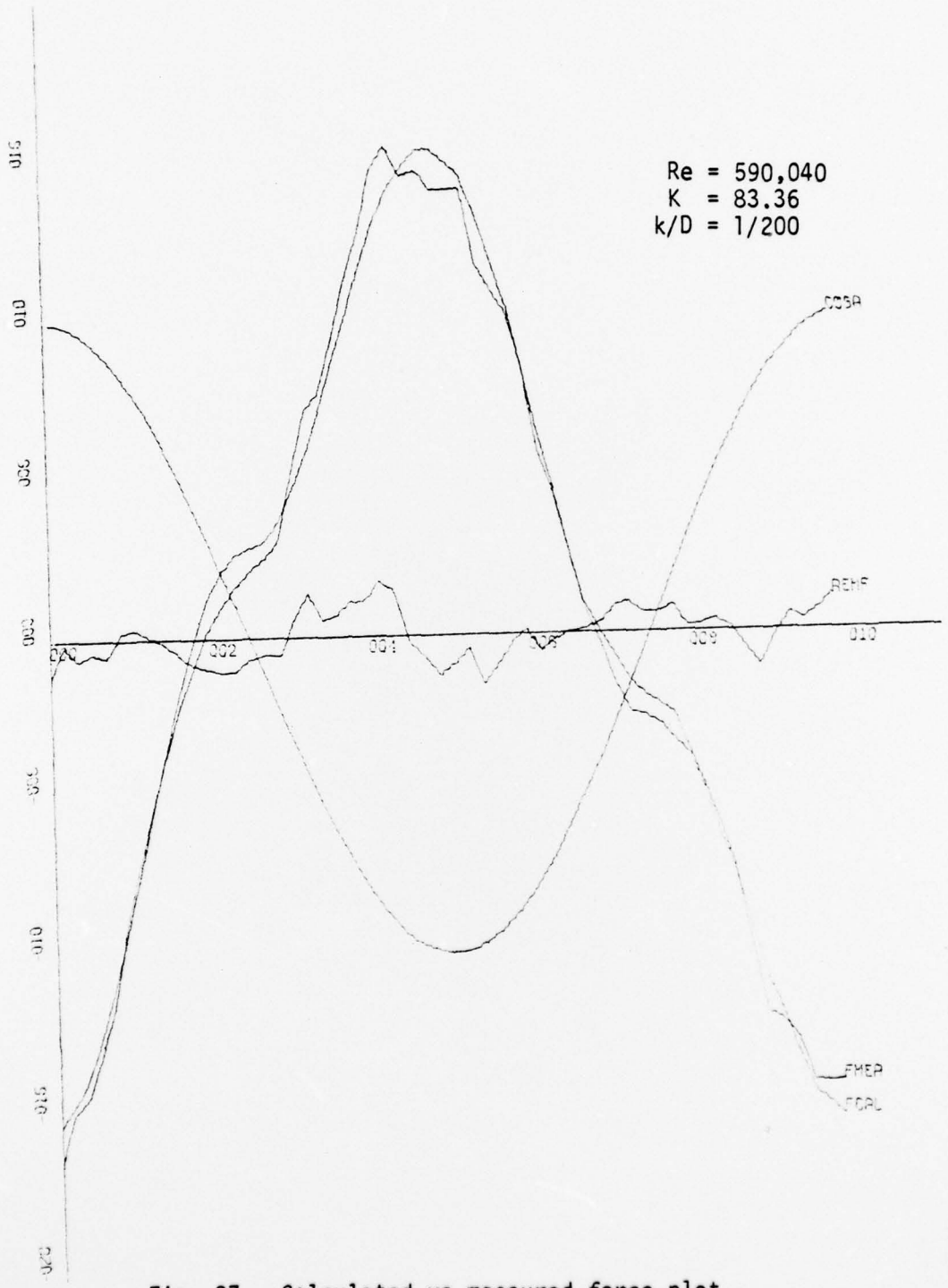

Fig. 27. Calculated vs measured force plot

V. CONCLUSIONS

The extensive investigation of the in-line forces on roughened circular cylinders in harmonic flow warrants the following conclusions:

1. The drag and inertia coefficients depend on the Reynolds number, the Keulegan-Carpenter number, and the relative roughness. The effect of size distribution and packing of the grains has been minimized by using only sand and applying it as uniformly as possible over the test cylinders;

2. The drag coefficient undergoes a drag crisis depending on the relative roughness and rises to an asymptotic value within the range of Reynolds numbers tested. The asymptotic values of the transcritical Reynolds number are larger than those corresponding to the smooth cylinder case. Furthermore, the larger the relative roughness, the larger is the asymptotic value of the drag coefficient;

3. The inertia coefficient also undergoes an 'inertia crisis' at Reynolds numbers corresponding to the 'drag crisis' at which C_m reaches a maximum value and then asymptotically decreases. The terminal values of C_m depend, as in the case of C_d, on K and k/D;

4. The predictions of the Morison's equation through the use of the Fourier-averaged drag and inertia coefficients are in excellent agreement with the measured forces in the range of K values smaller than about 10 and larger than about 20. In the neighborhood of K = 15, the effect of fractional vortex shedding [8] brings about lift-induced oscillations in the in-line force. The effect of these oscillations may

be incorporated into the Morison equation through the inclusion of at least two additional terms in the Fourier series;

5. The drag coefficients presented herein represent the maximum possible values for a given roughened cylinder because the wake is much better correlated than that behind a cylinder in the marine environment. Thus, a designer may choose drag coefficients somewhat below the values presented herein depending on the local conditions and ultimately on his personal judgment regarding the effect of reduced spanwise correlations.

VI. RECOMMENDATIONS

It is recommended that, among the many projects which could be undertaken, the effect of spanwise correlation be examined in detail. It would also be most desirable to repeat some of the experiments with cylinders roughened in the marine environment over a long period of time. It is through such investigations that one might eventually be able to understand the isolated effects of the three-dimensionality of the flow, the increase of the diameter of the connecting members of a structure, and the 'roughness' effect of the natural excrescences. Additionally, the investigation of wave slamming is of utmost importance.

APPENDIX - A COMPUTER PROGRAM

```
C ****************************************************************
C *                                                              *
C *                                                              *
C *  AVERAGE CM AND CD CALCULATIONS FOR CYLINDERS                *
C *                                                              *
C *  DIA = DIAMETER OF THE CYLINDER (FEET)                       *
C *  AMP = AMPLITUDE OF MOTION (FEET)                            *
C *  UMX = MAXIMUM VELOCITY DURING A CYCLE (FT./SEC.)            *
C *  CN = FORCE CALIBRATION FACTOR                               *
C *  FMM = MAXIMUM FORCE IN A CYCLE                              *
C *  DD = CHART CORRECTION FACTOR                                *
C *  CL = LENGTH OF CYLINDER (FEET)                              *
C *  XKC = PERIOD PARAMETER (UMX*PER/DIA)                        *
C *  REYNO = REYNOLDS NUMBER                                     *
C *                                                              *
C *                                                              *
C ****************************************************************C
C                                                                 C
C                    U - TUNNEL EXPERIMENTS                       C
C                                                                 C
C                                                                 C
C                                                                 C
C          THE FOLLOWING DATA ARE FOR THIS RUN                    C
C   DIA    ROUGH SIZE   TYPE   TEMP  VISCOSITY   DATE    RUNS     C
C 6.0 IN. 0.1027 IN. SAND 94 DEG. 0.00739   30JUL 101-113         C
C                                                                 C
C                                                                 C
C                                                                 C
      DIMENSION FORCE(55)
      DIMENSION UMTODX(75),REYNOX(75),CMX(75),CDX(75),CEL
     1SX(75),SIGMAX(75),CFMX(75),CLMX(75)
C
C     N = NUMBER OF DATA SETS FOR THIS RUN
C
      DO 100 I=1,N
      G=32.174
      READ(5,55) (FORCE(K), K=1,55)
      RHO=62.4/G
      PI=3.14159
      PIF=PI*PI*PI*PI
      CL=2.982
C
C     FOUR CARDS TO BE INSERTED HERE ARE:
C     ROD =          (ROUGHNESS TO DIAMETER, K/D)
C     CNU =          (VISCOSITY)
C     IBETA =          ( RE/K)
C     ITEMP =         (TEMPERATURE)
C
C
      ROD=0.0171
      CNU=0.00789
      IBETA=5904
      ITEMP=94
C
C     READ IN PARAMETERS WHICH CHARACTERIZE THE DATA SET
C
      READ(5,10)DIA,AMP,PER,NCARD,UMX,CN,FMM1,NRUN,DD
      WRITE(6,15)DIA,AMP,PER,UMX,CN,NRUN,DD
```

```
C
C     COMPUTE FORCE COEFFICIENTS
C
      C2=RHO*((UMX**2.0)/2.0)*DIA*CL
      Z1=(2*PER*PER)/(PI*PI*PI*DIA*DIA*CL*RHO*AMP)
      Z2=(-3*PER*PER)/(8*RHO*DIA*PI*CL*AMP*AMP)
      Z2LS=(-4*PER*PER)/(3*PI*PI*RHO*DIA*CL*AMP*AMP)
C
C     COMPUTE THE PERIOD PARAMETER AND REYNOLDS NO.
C
      XKC=2*PI*AMP/DIA
      REYND=(UMX*DIA)/CNU
C
C
      TIME=0.1*(DD-0.5)/PER
      SUM=0.0
      DEC=SQRT(UMX)
      DO 65 K=1,NCARD
      FORCE(K)=FORCE(K)*(1.0+((1.0+DEC/32.0)**2.0-1.0)*K/
     1NCARD)
      SUM=SUM+FORCE(K)
   65 CONTINUE
C
C
      FMEAN=SUM/NCARD
      DO 85 K=1,NCARD
      FORCE(K) =FORCE(K)-FMEAN
   85 CONTINUE
      FMAX=FMAX-FMEAN
      ZERO=0.0-FMEAN
C
C     INITIALIZE PARAMETERS
C
      CM=0.0
      CD=0.0
      CMLS=0.0
      CDLS=0.0
      FAA=0.0
      FBB=0.0
      FCC=0.0
      FDD=1.0
      FEE=0.0
      FFF=0.0
      DELTAT=0.10/PER
C
C     SUMMATION FOR CALCULATION OF CM AND CD INTEGRALS
C
      DO 200 K=1, NCARD
      F=CM*FORCE(K)
      CAP=CAP+F*F
      ALPHA=2*PI*TIME
      SINA=SIN(ALPHA)
      COSA=COS(ALPHA)
      FDELTA=DELTAT*F*SINA
      FCOSA=DELTAT*F*COSA
      FCLS=DELTAT*F*COSA*ABS(COSA)
      FAAC=2*PI*F*DELTAT*COSA*COSA*COSA*COSA*F
      FBBS=2*PI*F*F*COSA*ABS(COSA)*DELTAT*F
      FCCS=4*PI*F*SINA*COSA*ABS(COSA)*DELTAT*F
      FCLS=4*PI*F*SINA*SINA*DELTAT*F
      FDDS=2*PI*F*F*SINA*DELTAT*F
      FAA=FAAC+FAA
      FBB=FBBS+FBB
      FCC=FCCS+FCC
      FDD=FDDS+FDD
      FEE=FCLS+FEE
      FFF=FDELTA+FFF
      CM=FCOSA+CM
      CD=FCOSA+CD
      CMLS=FDELTA+CMLS
      CDLS=FCLS+CDLS
      TIME=TIME+DELTAT
  200 CONTINUE
```

```
C
C     MULTIPLY CM, CD BY FORCE COEFFICIENTS
C
      CM=Z1*CM
      CD=Z2*CD
      CMOC)=(PI**2*CM)/(2.0*C))
      CMLS=Z1*CMLS
      CDLS=Z2LS*CDLS
      CMFF=(Z1/2.0)*(FEE*FAA-FCC*FBB)/(FDD*FAA-FCC*FCC)
      CDFF=(-4.0*Z2/(3.0*PI))*(FEE*FCC-FDD*FBB)/(FDD*FAA-
     1FCC*FCC)
      IF( XKC.LT.CMOC)) GO TO 90
      CFSPP=CD+(PIF*CM*CM)/(4.0*C)* XKC* XKC)
      GO TO 91
   90 CFSPP=(PI**2*CM)/XKC
   91 CFRMS=SQRT((3.0*C)*CD/8.0)+(PIF*CM*CM)/(2.0*XKC*XKC))
      CFMAX=FMMM*CM/C2
      CARM=SQRT(CAR/55.0)
      CARMS=CARM/C2
C
C     INITIALIZE COEFFICIENTS FOR COMPUTATION OF FORCES
C
      ANGLE=0.0
      TIME=0.0
      ESQ=0.0
      EMFLS=0.0
C
C     COMPUTE MEASURED AND CALCULATED FORCES USING
C     THE COEFFICIENTS C1, C3
C
      DO 300 K=1,NCARD
      E=CM*FORCE(K)
      F=E/C2
      ALPHA=2.0*PI*TIME
      THETAL=((2.0)*PI)/360))*ANGLE
      C1=(ABS(COS(THETAL)))*COS(THETAL)
      C3=((PI**2)*DIA*SIN(THETAL))/(UMX*REF)
      E1=(CM*C3-CD)*C1)
      ELNEW=E1
      ELS=(CMLS*C3-CDLS*C1)
      EFOR=(CMFF*C3-CDFF*C1)
      ESQ=ESQ+E**2
      EMFLS=EMFLS+(E-E1)*(E-E1)
      ERME=ABS(E)-ABS(E1)
      ANGLE=ANGLE+30.0/PER
      TIME=TIME+DELTAT
  300 CONTINUE
      SIGMA=100.0*(SQRT(EMFLS/ESQ))
      WRITE(6,35)
      WRITE(6,40)CM,CD, XKC,REYNO,CMLS,CDLS,CMFF,CDFF,ZERO
      WRITE(6,42)
      WRITE(6,44) CFSPP,CFRMS,CFMAX,CARMS,SIGMA
      UNITDX(I)=XKC
      REYNDX(I)=REYNO
      CMX(I)=CM
      CDX(I)=CD
      CFMX(I)=CFMAX
      SIGMAX(I)=SIGMA
      CDLSX(I)=CDLS
  100 CONTINUE
      WRITE(6,915)
      WRITE(6,900) DIA,ROD
      WRITE(6,901) TEMP,BETA
      WRITE(6,902)
      DO 400 I=1,N
      WRITE(6,903) UNITDX(I),REYNDX(I),CMX(I),CDX(I),CDLSX(
     1I),CFMX(I),SIGMAX(I)
  400 CONTINUE
   10 FORMAT(3F8.4,I3,4F8.4,I8,F4.1)
```

```
 15 FORMAT('0',2X,'DIA=',F8.4,2X,'AMP=',F8.4,2X,'PER=',
    1F8.4,2X,'UMX=',F8.4,2X,'CM=',F8.4,20X,'MRUN=',I6,
    2'      LO=',F4.1)
 35 FORMAT('0',7X,'CM=',7X,'CD=',7X,' KC =',7X,'REYNO=',7X,
    1'CMLS=',7X,'CDLS=',7X,'CMFF=',7X,'CDFF=',7X,'ZERO=')
 40 FORMAT('0',6F12.4,3F12.4)
 42 FORMAT('0',6X,'CFSPP=',6X,'CFRMS=',6X,'CFMAX=',6X,'C
    1ARMS=',6X,'SIGMA=')
 44 FORMAT('0',5F12.4)
 55 FORMAT(11F6.1)
    WRITE(6,905)
900 FORMAT('1',7X,'CYLINDER DIAMETER =',F7.4,3X,'SURFACE
    1 ROUGHNESS(E/D) =',F7.5,/)
901 FORMAT(8X,'TEMPERATURE =',I3,13X,'BETA =',I5,//)
902 FORMAT(8X,'UMTOO',5X,'REYNO',4X,'CM',4X,'CD',5X,'CDLS'
    1,4X,'CFMX',3X,'SIGMA',3X,'CLMX',/)
903 FORMAT(6X,F7.2,3X,F7.3,1X,F6.2,1X,F5.2,1X,F6.2,2X,F6.
    12,2X,F6.2)
904 FORMAT(F7.2,F7.3,5F7.2)
905 FORMAT('1')
999 STOP
    END
```

LIST OF REFERENCES

1. Sarpkaya, T., "Vortex Shedding and Resistance in Harmonic Flow about Smooth and Rough Circular Cylinders at High Reynolds Numbers," Naval Postgraduate School Technical Report No. 59SL76021, Monterey, Calif., 1976.

2. Collins, N. J., "Transverse Forces on Smooth and Rough Cylinders in Harmonic Flow at High Reynolds Numbers," M. S. and Mechanical Engineer Thesis, Naval Postgraduate School, Monterey, Calif., 1976.

3. Fage, A. and Warsap, J. H., "The Effects of Turbulence and Surface Roughness on the Drag of a Circular Cylinder," Aero. Res. Comm., London, Reports and Memoranda No. 1283, 1929.

4. Achenbach, E., "Influence of Surface Roughness on the Cross-flow around a Circular Cylinder," Jour. of Fluid Mechs., Vol. 46, pp. 321-335, 1971.

5. Morison, J. R., et al., "The Force Exerted by Surface Waves on Piles," Petroleum Trans., Vol. 189, pp. 149-157, 1950.

6. Keulegan, G. H., and Carpenter, L. H., "Forces on Cylinders and Plates in an Oscillating Fluid," Journal of Research of the National Bureau of Standards, Vol. 60, No. 5, Research Paper No. 2857, pp. 423-440, May 1958.

7. Schlichting, H., Boundary-Layer Theory, McGraw-Hill Book Company, New York, Sixth Edition, pp. 586-587, 1968.

8. Sarpkaya, T., "In-line and Transverse Forces on Cylinders in Oscillating Flow at High Reynolds Numbers," Proceedings of the Offshore Technology Conference, Paper No. OTC-2533, May 1976.

9. Fage, A. and Falkner, V. M., "Further Experiments on the Flow Around a Circular Cylinder," Aero. Res. Comm., London, Reports and Memoranda No. 1369, 1931.

INITIAL DISTRIBUTION LIST

	No. Copies
1. Library, Code 0142 Naval Postgraduate School Monterey, Calif. 93940	2
2. Department Chairman, Code 69 Department of Mechanical Engineering Naval Postgraduate School Monterey, California 93940	1
3. Professor T. Sarpkaya, Code 69SL Department of Mechanical Engineering Naval Postgraduate School Monterey, California 93940	5
4. Lieutenant Steven R. Evans, USN c/o Supervisor of Shipbuilding Conversion and Repair, USN Pascagoula, Mississippi 39567	2
5. Defense Documentation Center Cameron Station Alexandria, VA 22314	2